



This is a repository copy of *Factors influencing the fire dynamics in open-plan compartments with an exposed timber ceiling*.

White Rose Research Online URL for this paper:

<https://eprints.whiterose.ac.uk/190809/>

Version: Accepted Version

Article:

Nothard, S., Lange, D., Hidalgo, J.P. et al. (4 more authors) (2022) Factors influencing the fire dynamics in open-plan compartments with an exposed timber ceiling. *Fire Safety Journal*, 129. 103564. ISSN 0379-7112

<https://doi.org/10.1016/j.firesaf.2022.103564>

Article available under the terms of the CC-BY-NC-ND licence
(<https://creativecommons.org/licenses/by-nc-nd/4.0/>).

Reuse

This article is distributed under the terms of the Creative Commons Attribution-NonCommercial-NoDerivs (CC BY-NC-ND) licence. This licence only allows you to download this work and share it with others as long as you credit the authors, but you can't change the article in any way or use it commercially. More information and the full terms of the licence here: <https://creativecommons.org/licenses/>

Takedown

If you consider content in White Rose Research Online to be in breach of UK law, please notify us by emailing eprints@whiterose.ac.uk including the URL of the record and the reason for the withdrawal request.



eprints@whiterose.ac.uk
<https://eprints.whiterose.ac.uk/>

FACTORS INFLUENCING THE FIRE DYNAMICS IN OPEN-PLAN COMPARTMENTS WITH AN EXPOSED TIMBER CEILING

Sam Nothard¹, David Lange¹, Juan P. Hidalgo¹, Vinny Gupta², Martyn S. McLaggan³, Felix Wiesner¹, Jose L. Torero⁴

1. The University of Queensland, Australia; 2. The University of Sydney, Australia, 3. The University of Sheffield, UK, 4. University College London, UK

ABSTRACT

Fires in open plan compartments have been the subject of much research over the past decade. This article presents results from an experimental study conducted to explore factors that influence fire dynamics in open-plan compartments with an exposed timber ceiling.

A reduced scale testing methodology is proposed and supported by contrasting observed fire behaviour at small scale with large-scale experiments reported in the literature. The reduced-scale experiments highlight the complexity of the fire dynamics. Factors which govern the behaviour include the ignition and self-extinction of the timber; the role that the timber plays in accelerating the transition from Mode 3 (travelling) to Mode 1 (fully developed) behaviour; the ignition and self-extinction of timber which is in a downward facing orientation; the thermal inertia of the ceiling material.

Results demonstrate that: different fire modes observed in large scale compartments occur in large scale compartments with combustible timber ceilings; ceiling intrusions influence the fire; and factors that influence the response of timber in open plan compartment fires can, to a large extent, be explained by existing knowledge extracted from bench scale testing and compartment fires with non-combustible linings.

Keywords: Timber, open plan compartments, compartment fire dynamics, CLT

1 INTRODUCTION

The fire dynamics in small compartments with non-combustible linings were characterised throughout the 20th century, leading to the development of a scientific framework that characterises this behaviour [1, 2]. In particular, emphasis was placed on characterising post-flashover compartment fires, specifically so-called ventilation-controlled or Regime I fires where the control volume is considered well-stirred and the flow field is described by a hydrostatic exchange of mass at the compartment opening [3]. Kawagoe showed that in this case the burning rate is proportional to the product of the opening area and the square root of the opening height ($A_0\sqrt{H_0}$), which is commonly referred to as the ventilation factor [4]. This parameter closes the global energy balance for Regime I type compartment fires, with simplified expressions proposed for the burning rate and gas temperatures.

However, these expressions break down for compartments with larger openings and geometries, where the assumptions of hydrostatic flow and temperature homogeneity within the compartment do not hold. This regime of fires has often been classically referred to as fuel-controlled or Regime II and is very difficult to characterise owing to the non-uniform conditions that arise from complex momentum-driven flow fields defined by the interplay of the compartment and fire characteristics. These fires were originally thought to be less onerous as peak gas temperatures were found to be smaller than in Regime I fires [5]. Nonetheless, the compartment fire framework was limited in its applicability and so long as compartments were not designed in such a way that they would result in Regime II fires then this would not be an issue.

However the increasing usage of large open-plan spaces in contemporary buildings, which are likely to be subject to Regime II fires, indicates that this limit of applicability has not been respected. Correspondingly, some limited research has been undertaken to try to characterise the fire dynamics and develop appropriate design methods [6]. However existing examples of open plan compartments have for the most part relied on fire safety design taking advantage of the apparently more onerous conditions of the Regime I fire as opposed to considering the possible Regime II fires. In such compartments, it is unlikely for the compartment to reach post-flashover conditions over the entire floor plate, and the fire is likely to exhibit one of a number of modes determined by the ratio of the flame spread rate, V_S , to the burnout rate, V_{BO} , of the fuel [7 - 9]. The three modes of fire spread as identified are summarised in Table 1.

Table 1 – Characteristic flame spread modes.

Characteristic Mode	Fire Behaviour Description	Value
Mode 1 (fully developed)	Extremely rapid to instantaneous increase in flame front	$V_S/V_{BO} \rightarrow \infty$
Mode 2 (growing)	The flame front increases faster than the burnout front	$V_S/V_{BO} > 1$
Mode 3 (travelling)	The flame front and burnout front move at the same constant rate	$V_S/V_{BO} \approx 1$

The authors have described and analysed these modes in great detail, with simplified descriptions of the flame spread and burnout processes defining each mode, and the thresholds leading to transitions from one mode to another provided [10]. Mode 3 occurs for compartment fires with very large advection heat losses, meaning that most of the heat released by the fire is carried away by convective flows and therefore the smoke layer is unable to provide any meaningful preheating of the fuel, and thus flame spread and burnout is driven primarily by the fuel characteristics. For Mode 2, a sufficiently hot and deep smoke layer extending above the fuel bed preheats the fuel ahead of the flame front towards an ignition temperature, thereby accelerating fire spread. For Mode 1, a critical heat flux for ignition of the fuel is exceeded by the conditions inside of the compartment and the fuel undergoes very rapid flame spread. The complexity of this behaviour has required extensive study over a number of years, and a final proposed framework is only now in the process of being published [11]. In this framework, there are still significant limitations, uncertainties and further work required, and the characterisation of Regime II fires remains a work in progress although the level of understanding is significantly better than when the compartment fire framework was first proposed or when Torero et al [6] revisited these concepts.

Efforts have been made to develop simple engineering tools to estimate the thermal boundary condition for the case where the ratio of spread rate to burnout rate, V_S/V_{BO} is at unity ($\frac{V_S}{V_{BO}} \approx 1$). Such methodologies, developed for the purposes of structural design are described by Stern-Gottfried et al. and predate the identification of the above modes [12,13]. The outcome of these efforts is termed the Travelling Fire Methodology, and numerous high-profile fires can be cited, most notably the World Trade Centre towers (1, 2 & 7), as evidence of this behaviour. The framework has been extended and modified in various ways [14 - 16], but the basic premise includes the localised fire plume impinging a ceiling yielding large thermal exposures (termed the ‘near field’), and a hot gas layer or ceiling jet remote from the fire plume that is preheating the compartment (the ‘far field’). The fuel in each area is finite, and the model assumes that the progression of the flame front and burnout front are constants, and thus the size of the area of localised burning is constant. Across the compartment this leads to an exposure which is highly heterogeneous and capable of lasting long periods of time, far longer than the fire exposure that would be expected in small compartments. These methodologies, which were not originally intended to be predictive but rather to be used to solicit a range of structural responses when subject to non-uniform heating, show their weaknesses when compared with the limited relevant experimental data available. This data suggests that the heat fluxes experienced by a structure exposed to a fire which travels according to this definition are likely to be significantly lower than those which are estimated based on these methods [17]. Whilst this highlights the inherent conservatism in these methods it also motivates a more thorough scrutiny.

One area of significant further interest is the influence of combustible ceilings on the above behaviour. With timber as a construction material experiencing rapid growth in its use at the moment as a result of strong environmental credentials and a drive for an improved end user experience in offices and residential developments. This growth has been enabled by the development of both engineered timber products and the structural engineering knowledge required to build taller timber buildings or new structural forms from timber. Nevertheless, engineered timber construction, in particular when there is a desire to express this architecturally, poses a significant challenge for the fire safety design of buildings [18], not least of which because it introduces combustible surfaces into compartments [19, 20]. This architectural expression is possible in many jurisdictions through the use of engineering methods in performance based regulatory environments, and is likely to become more and more common.

However, much of the work ongoing to understand the behaviour of timber in compartment fires originates from compartments that are approximately cubic and where post-flashover fire conditions and a Regime I fire are all but guaranteed. This has led to the demonstration of the concept of self-extinction of burning timber in compartment fires, defined as the process whereby the exposed CLT ceiling ceases to continue flaming upon removal of the applied external heat flux, and the identification of criteria for this [21 - 24]. Further work has also been done to study the applicability of the compartment fire framework when exposed timber is present [20, 25 - 28]. Crucially, despite developments in the theory of fire dynamics and fire spread in open-plan compartments, these theories have not been fully extended to compartments with exposed timber surfaces, mostly owing to the lack of systematic data to characterise these fires. There is therefore a need to understand the impact that exposed timber surfaces in a large open plan compartment will have on the fire dynamics. Notable tests which have been conducted and which explore the behaviour of timber in similar geometries include: the Structural Timber Association special interest group tests which aimed to determine whether glue line integrity failure was a pre-requisite for self-extinction [29]; and work conducted by Arup, CERIB and Imperial College London's HAZELAB which explored the impact of opening factor on fire spread in open plan timber compartments [30]. The former was conducted in a compartment of 4.5 m x 9.5 m floor plan and demonstrated that self-extinction can occur even with a large amount of char fall-off; and the latter, based on currently available information, demonstrated in a compartment of 174 m² a very fast spread rate of fire. The potential impact of such combustible ceilings on open-plan compartment fire dynamics was also demonstrated in the Malveira Fire Test - where one half of the compartment, on one side of the protrusion of the middle beam had a cork lined ceiling the ignition of which coincided with a very rapid transition from Mode 2 to Mode 1 [8].

This paper contributes to addressing this research gap through a series of 6 fire experiments conducted in a reduced-scale compartment with both non-combustible and combustible ceiling linings. This systematic study of the influence of exposed timber on the fire dynamics in open plan compartments is entirely novel. The test setup is shown in Figure 1 during one of the tests. Some results from this study have been presented elsewhere [31], however this article provides a more detailed presentation, analysis and discussion. Scaled-down testing is implemented in this work as a means of systematically exploring specific behaviour for the identification of phenomenon which may need to be explored in more detail at a large scale. In these tests, the similarity that is sought is the demonstration of the same fire modes as are observed in full scale tests of similar geometry. The assumption is that if the behaviour observed in terms of fire spread modes and the factors which govern that for the tests with non-combustible ceiling is the same at the two different scales then the same could be said for tests with combustible ceilings. The results are therefore more qualitative than quantitative and are intended as phenomenologically informative. This paper is thus intended to identify relevant phenomenon and processes that may govern this problem.



Figure 1. External view of the test setup during flat ceiling exposed CLT test.

2 METHODOLOGY

Scale testing is implemented in this work as a means of systematically exploring specific behaviour for the identification of phenomenon which may need to be explored in more detail at a large scale. The problem discussed in this article requires geometric scaling as well as ultimately consideration of the scaling of the relevant fire dynamics. However, scaling fire phenomena requires preservation of too many non-dimensional groups to encapsulate similarity between the model and prototype [32]. Since complete scaling is not viable, partial scaling is required and the modelling prerequisite used in this paper is that the physical model (the scaled model) is ‘similar’ to the prototype (full scale) in the sense that there is a correlation between the general response of the two systems to equivalent stimuli events. Therefore, for the series of tests reported in this paper, the fire source (heat release rate) and the compartment geometry are both scaled whilst other aspects of the fire dynamics, such as time, momentum, etc. are assumed to be phenomenologically similar in the scaled test but are not directly preserved through the scaling analysis since this would inevitably disable any attempt to preserve any of the relevant non-dimensional parameters. Phenomenological similarity is, therefore, the only argument in support of the choice of scale. This is a limitation that the authors recognize and that defines the qualitative nature of these results.

2.1 Compartment configuration

Geometric scaling is typically straight forward and uses a length scale (l) to define the geometric relationship between the full-scale prototype and scale model. The experimental compartment was thus designed to approximate a 1/8 reduced scale geometric configuration of large-scale experiments in the literature, namely the Malveira Fire Test [8], the ETFT experimental campaign [7] and the Guttasjön Fire Tests [9, 33]. The aspect ratio is also similar to that of the floor plate of International House, a multi-storey CLT building in Sydney. Table 2 outlines the compartment geometry in comparison to previous full-scale open plan test compartments. These aspect ratios lend themselves towards one-dimensional flame spread.

This paper will make no further attempt at developing scaling arguments to justify the 1/8 geometric ratio used. This was defined only on the basis of the capacity of the available hood.

Table 2 – Scaled compartment geometry comparison with full scale tests.

Compartment	Length [m]	Aspect ratio (Length /Depth)	Depth [m]	Aspect ratio (Depth / Height)	Height [m]

Scaled 1/8 test compartment	2.22	5.6	0.80	2.0	0.40
Full scale equivalent compartment	17.80	5.7	6.40	2.1	3.12
Malveira Fire Test [8]	21.00	7.4	4.70	1.6	2.85
Edinburgh Tall Building Fire Tests (ETFT) [7]	17.80	8.9	4.90	2.5	2.00
Guttasjön Fire Tests (GFT) [9, 33]	18.00	6.0	6.00	2.0	3.00

The experimental compartment had a single large opening for ventilation along the longitudinal front of the compartment, similar to the compartments in references [7] and [8] (the compartment in references [9] and [33] had openings on both of the longer sides and exhibited Mode 3 and Mode 2 behaviour only). The material used for the compartment floor and walls was vermiculite board (with a density of 375 kg/m³, specific heat capacity of 0.94 kJ/kgK, and a thermal conductivity of 0.12 W/mK measured at 200 °C).

The ceiling lining was varied between the different tests. Three baseline tests were conducted using a non-combustible ceiling constructed with 16 mm thick plasterboard (with a density reported by the manufacturer of 780 kg/m³, specific heat capacity of 1.09 kJ/kgK a thermal conductivity of 0.24 W/mK; all at ambient conditions) covered in 5 mm thick ceramic wool (Superwool Paper Insulation) on the exposed surface (ceramic wool with a density of 96 kg/m³, a specific heat capacity of 1.13 kJ/kgK, and a thermal conductivity of 0.09 W/mK at 400 °C). Since ceramic wool was only fastened at fixed points, with relatively poor contact with the plasterboard, the thermal inertia of the non-combustible ceiling configuration can be estimated to be that of the ceramic wool: 0.00976 kJ²/m⁴K²s.

The entire ceiling was then substituted for three further tests with a 125 mm thick Radiata Pine CLT ceiling (comprised of three lamellae of thickness 45, 35, and 45 mm with average density of 460 kg/m³ – representing a typical structural CLT product on the market in Australia, and an average moisture content on the days of the tests of 9.8 % based on electrical resistivity measurement).. Based on the range of thermal properties of wood reported in Eurocode 5 [34] the thermal inertia of the combustible ceiling can be expected to vary between 0.0862 kJ²/m⁴K²s at ambient temperature and 0.0676 kJ²/m⁴K²s at 800 °C - a factor of between 7 and 9 higher than for the non-combustible ceiling. In the tests with combustible ceilings the entirety of the ceiling was exposed, with none of the surface area of the timber protected. No other changes were made to the compartment.

Different compartment configurations comprised intrusions in the ceiling which were made from the same vermiculite board that was used for the floor and compartment walls. These intrusions comprised a beam inserted along the top of the opening of the compartment (an edge beam); and a beam inserted along the short axis centreline of the compartment (middle beam). The intrusions serve, in these tests, as a mechanism to enable some level of smoke accumulation, providing an opportunity to further explore the role of optical thickness as a governing phenomenon for radiative feedback. Both of these intrusions had a depth of 70 mm. Table 3 provides a summary of the opening and ceiling characteristics for each test configuration. The position of the ceiling intrusions is shown in Figure 2. Given the practical value of understanding the role of intrusions (given that these will always exist in real buildings), the observations pertaining this aspect of the study are purely qualitative and only aim at generating evidence that could serve to establish the need for further study.

Table 3 – Compartment opening characteristics.

Test Configuration	Configuration 1	Configuration 2	Configuration 3
Description	No edge beam	Edge beam	Edge & middle beam
Opening Width [m]	2.2	2.2	2.2
Opening Height [m]	0.4	0.33	0.33
Opening Area [m ²]	0.88	0.726	0.726

Smoke Reservoir Volume [m ³]	0	0.126	2 x 0.062
------------------------------------------	---	-------	-----------

In the presentation and discussion of the results of this testing program, the following labelling is adopted to differentiate between the test variables:

1. The different ceiling linings– indexed by B (Baseline) and C (CLT); and
2. The different compartment configurations – indexed by 1 (flat ceiling), 2 (edge beam) and 3 (edge and middle beam).

In total, therefore, a series of six (6) experiments were carried out, table 4 provides an overview of the experimental program.

Table 4 – Testing matrix.

Test No.	Ceiling	Edge Beam	Middle Beam
Baseline Tests			
B1	non-combustible	none	none
B2	non-combustible	present	none
B3	non-combustible	present	present
CLT Tests			
C1	CLT	none	none
C2	CLT	present	none
C3	CLT	present	present

2.2 Instrumentation

Instrumentation in each of the tests was designed to enable a quantification of the fire dynamics and the thermal environment for each test. The layout of the instrumentation is shown in Figure 2. In summary:

- The compartment was placed underneath a hood with a calorimeter to collect combustion products from the opening and record the HRR through carbon dioxide generation calorimetry.
- A load cell was placed under each end of the compartment to record the total mass loss evolution of the compartment in time.
- Eight thermocouple trees were placed along the centre line of the compartment, each having 7 inconel sheathed Type-K thermocouples of external diameter 1.5 mm; positioned 0.13, 0.18, 0.23, 0.28, 0.33, 0.355 and 0.37 m from the floor of the compartment. The thermocouples were more closely spaced towards the ceiling to determine how the smoke layer and ceiling jet varied as the ceiling edge and middle beam were introduced. Thermocouple temperatures are not reported in this paper, although the presence of the thermocouple trees is noted here for completeness. A discussion of these results is intended to follow in a future publication.
- Sheathed Type-K thermocouples having a diameter of 1.5 mm were inserted into the CLT ceiling when this was included in the test. These were positioned in eight groups along the centre line of the ceiling. Each group had three thermocouples inserted at depths of 10, 20 and 45 mm from the exposed surface. The holes were drilled from the non-exposed surface using a CNC machine, at 90 degrees to the expected isotherms, in order to maintain accuracy of the drilling depths and locations. As with the thermocouple temperatures in the gas phase, these results are not discussed in this paper. An initial analysis has been presented [31], with further analysis planned.
- Thin skin calorimeters (TSCs) were used to measure the incident heat flux on the floor and ceiling of the compartment. These were placed along either side of the fuel bed and along the centre line of the compartment ceiling. A total of 16 were used on the floor (8 either side) and 9

along the ceiling. The TSCs were comprised of vermiculite board which had a thickness of 40 mm and an overall diameter of 50 mm with a 10 mm diameter Inconel disc on the measuring surface; these were manufactured and calibrated according to the description given in [35]. Reference [35] also describes sources of uncertainty and error in the use of TSC's, which are shown to result in a difference of ca. 6 % of measured heat flux at an irradiance of 80 kW/m² during calibration studies. The TSCs that were installed on the ceiling were mounted flush with the ceiling surface. The TSCs installed along the floor were mounted in 75 mm deep aerated concrete blocks such that they were flush with the top layer of the wood crib fuel bed.

In addition to the above, the flame front and burnout location of the fire was determined based on video footage recorded for each test. Processing of the videos took frames from set time intervals as the fire spread with the flame front and burnout location determined based on a reference distance to scale the video frames. 30 second intervals were initially used for the flame spread. As the fire grew a smaller interval of 15 seconds was used to track the flame front. The analysis relied on manual selection of the flame front and burnout front for each key frame. Once the fire was fully developed, the fuel load burnt out approximately simultaneously across the compartment resulting in an indeterminate burnout front as the remaining fuel was consumed at a relatively homogenous rate.

2.3 Fuel load

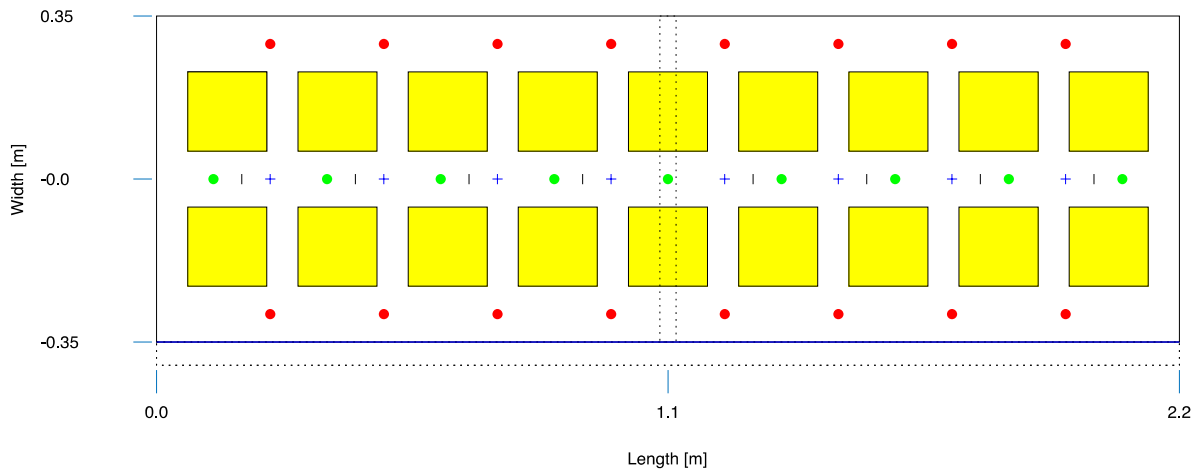
Wood cribs were used as the movable fuel load. The sticks used in these tests had a square cross section of 25 mm and a length of 170 mm. These were arranged in 3 layers with 4 sticks per layer, resulting in a spacing of 23.3 mm, ensuring a porosity > 0.1, and an exposed area of timber, A_b , in the crib of 0.184 m². The measured heat of combustion, ΔH_c , of the wood sticks was determined to be 12.4 MJ/kg and the mass loss rate per unit area, \dot{m}'' , of each stick was determined to be 7 g/m²s – both based on iCone testing. The heat release rate, \dot{Q} , for a single wood crib was estimated to be 15.95 kW (based on the relationship $\dot{Q} = \dot{m}\Delta H_c$ where the mass loss rate, \dot{m} , is determined from $\dot{m} = \dot{m}''A_b$). The wood cribs had a mass of approximately 780 g each. The spacing size of the sticks in the crib is selected to ensure that the crib porosity is sufficiently large to guarantee that crib burning rate is not controlled by the porosity of the crib [36], but instead by the crib geometry and thermal feedback from the compartment [37].

The heat release rate of these wood cribs scales to a 2.9 MW fire for each crib (according to the equation $\frac{\dot{Q}_M}{\dot{Q}_F} = \left(\frac{L_M}{L_F}\right)^{5/2}$, where $\frac{\dot{Q}_M}{\dot{Q}_F}$ is the ratio of the heat release rate in the model crib to the heat release rate of a full scale crib and $\frac{L_M}{L_F}$ is the ratio of the length of the model crib to the full scale crib [32]).

A total of 18 wood cribs were used in each test, arranged in two rows of 9 either side of the longitudinal centreline of the compartment, resulting in a total movable fuel mass of 14.054 kg. The total energy available based on the product of the heat of combustion and the mass of movable fuel is estimated at 173.6 MJ.

Preliminary testing found a spacing of 5 cm between wood cribs was sufficient to ensure auto-ignition of consecutive wood cribs. Ignition of the fuel bed was at the left-hand side in the orientation shown in Figure 2. To achieve ignition of the wood cribs a small pan containing 30 ml Kerosene was placed underneath both of the left most cribs and was ignited first. The fire was allowed to freely propagate from the ignition point along the fuel-bed.

Plan view



Elevation

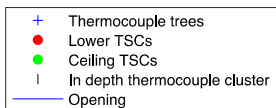
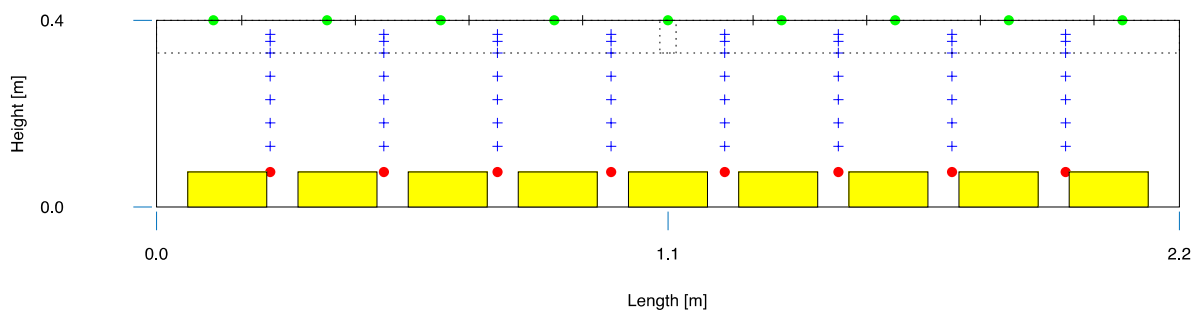


Figure 2 – Ceiling intrusions and sensor locations throughout the compartment in plan view and elevation view (note that the fuel layout is shown in yellow) (not to scale)

3 RESULTS AND ANALYSIS

In the following sections, the test results are discussed in terms of the mass loss rate, the heat release rate, the flame front and burnout location, and finally the behaviour of the CLT in terms of ignition and self-extinction (in this instance referring to the cessation of flaming combustion).

To aid in the interpretation and understanding of the results, a timeline of events observed in all 6 tests is shown in Figure 3. The figure shows the time to each row of cribs fully flaming (defined in this paper as the time at which fire had spread across the entire upper surface of one of the two cribs in each row) in each test and the time to burnout of each wood crib; both based on observations made during the tests. The general observation is that the tests that do not include a timber ceiling (B1, B2 and B3) follow similar characteristics, but the presence of intrusions accelerates the rate of spread of the fire over the cribs. The edge beam intrusion having the greatest effect while the middle beam intrusion concentrating the effect on Rows 1 to 3. This is expected, given that the intrusions allow a smoke layer of increased depth, thus increased optical thickness and increased radiative feedback.

For the 3 CLT ceiling lined tests, Figure 3 also shows the time to first observed ignition of the ceiling; the time over which the CLT ceiling is burning without interruption. Also identified is the time at which the first local occurrence of self-extinction of the CLT ceiling is observed – defined based on the visual observation of local-extinction in any one area of the ceiling.

In its initial stages the fire produced by the cribs, Row 1 burning, is not capable of igniting the ceiling, after Row 2 ignites, and particularly Row 3, the first visual observations of ignition of the ceiling occur. Ignition occurs above the burning cribs, with the first ignition events incapable of sustaining flame propagation across the ceiling. However, after some time, the spread of the flames over the entire ceiling is rapid with ignition of the ceiling occurring at approximately 56, 52 and 41 minutes. This continuous burning is characterised by flames rapidly spreading across the ceiling surface (taking only a few seconds to spread from one side of the compartment to the other), consistent with the ceiling flame spread experiments reported by Hasemi et al [38]. There is a short delay between ignition of the ceiling and spread across the fuel bed. This observation is consistent with published large-scale results [8]. The ceiling continues to burn until Rows 1 to 3 are mostly consumed. By the time these three rows show no flaming, self-extinction of the timber ceiling becomes evident above the consumed fuel. Upon consumption of the remaining wood cribs the self-extinction follows the passage of the burnout with a delay of at least 10 minutes after the last of the wood cribs had burnt out until complete extinction.

Images of the compartment at different stages of the fire development are provided in Appendix A. Table A1 shows images from the baseline tests and Table A2 shows images from the CLT tests. Times at which these images are taken are provided, as is the behaviour observed at these times, based on the analysis that will be presented in subsequent sections of this paper.

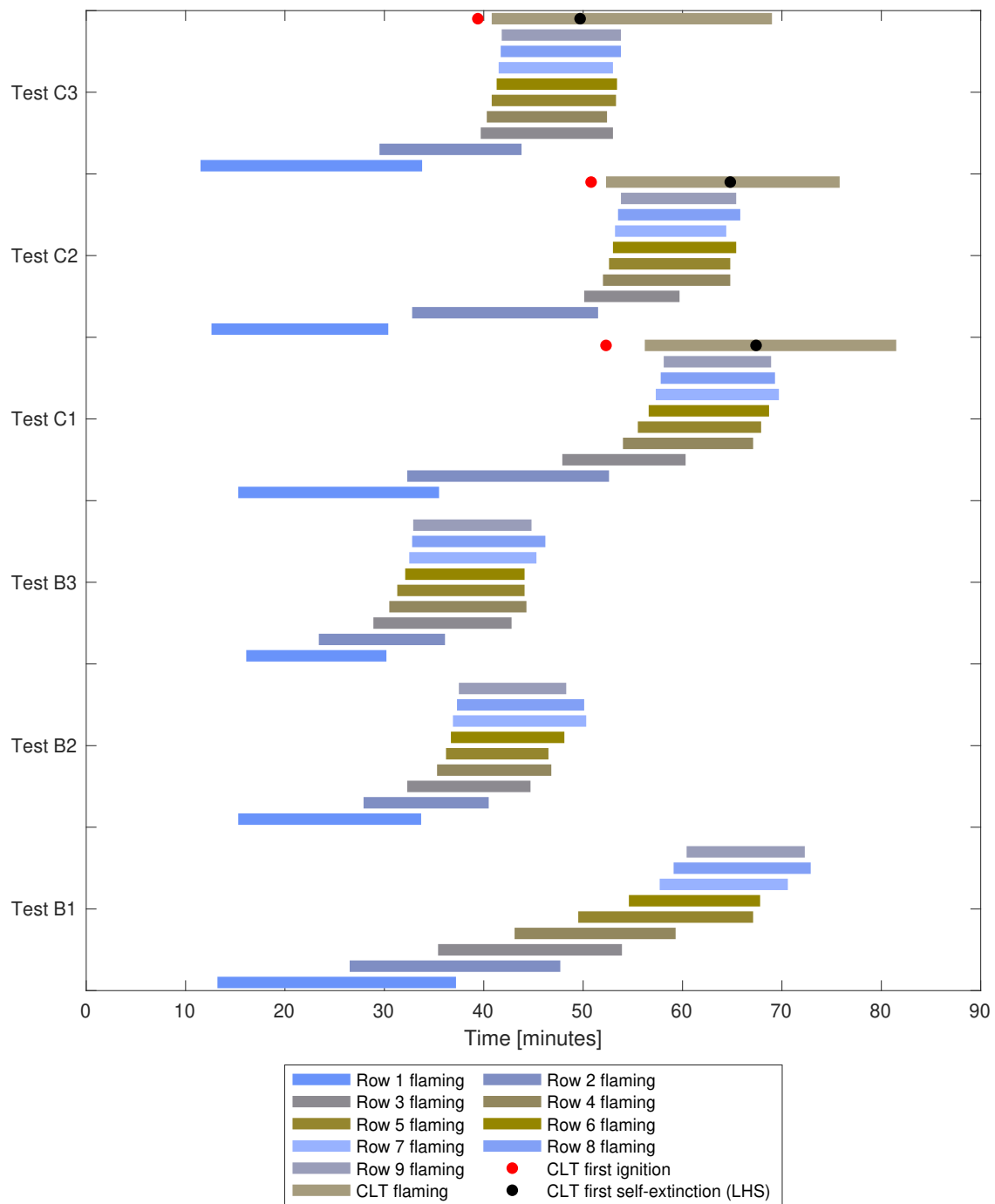


Figure 3. Timeline of ignition of each element in the 6 tests.

3.1 Mass loss and spread rates

Since the entire test setup was placed on load cells, the mass loss rate reported is based on the combined mass loss of both the wood crib inside of the compartments in all 6 tests and includes the CLT ceiling in tests C1 to C3. Mass loss rates from the baseline tests are reported in Figure 4. Mass loss rates from the CLT tests are reported in Figure 5.

In the results presented in this paper, the presence of the different Modes is defined through the mass loss rate. It has been shown before for continuous cribs that the total burning area (determined based on

video analysis as the difference of the flame and burnout fronts) is directly correlated to the crib burning rate [36]. For a Mode 3 fire, with $V_S/V_{BO} \approx 1$, the mass loss rate, dM/dt , is approximately constant as a function of time, i.e. $d^2M/dt^2 \approx 0$ g/s/min. Whereas for a Mode 2 fire and a Mode 1 fire, the mass loss rate increases with time as the flame front accelerates. Times for the transition between the different modes are therefore based on this criterion, with the following arbitrary limits applied:

- The transition from Mode 3 ($V_S/V_{BO} \approx 1$) to Mode 2 ($V_S/V_{BO} > 1$) is defined once $d^2M/dt^2 > 0.13$ g/s/min and without dropping below zero again before the burnout of the wood cribs (the above 0 threshold for the transition from Mode 3 to Mode 2 is intended to filter out noise that arises from taking the second derivative of the signal response).
- Transition from Mode 2 ($V_S/V_{BO} > 1$) to Mode 1 ($V_S/V_{BO} \rightarrow \infty$) in the baseline tests, B1 – B3 is deemed to have occurred when $d^2M/dt^2 > 0.5$ g/s/min, with the same caveat. The same criteria cannot be applied for tests C1 – C3 since the mass loss rate includes also the mass loss from the CLT ceiling and therefore the time to transition from Mode 2 to Mode 1 is based on observations of the increased flame spread rate inside of the compartment. This is seen in the tests reported herein to correspond with a peak in d^2M/dt^2 , which can be explained based on the fact that the transition from Mode 2 to Mode 1 is accompanied by a sudden increase in mass loss rate of the ceiling and the movable fuel load, which stops growing so rapidly as the char layer forms in the ceiling.

These limits serve only to aid consistent interpretation and visualisation of the results using the inequalities defined in Table 1 and are not intended to have any physical meaning.

Average mass loss rates in Mode 3 for all tests are very similar across all the experiments (B1 – 0.9 g/s, B2 – 0.7 g/s, B3 – 0.9 g/s, C1 – 1.1 g/s, C2 – 1.0 g/s, C3 – 1.1 g/s). Mass loss rate in Mode 2 peaks at between 4 and 6 g/s in the baseline tests, and although it is difficult to determine in the CLT tests since the transition between Mode 2 and Mode 1 occurs so quickly it is of a similar value when the criteria for transition between Mode 2 and Mode 1 are applied. In Mode 1, the baseline tests B2 and B3 have a mass loss rate which peaks at around 25 g/s; whereas the CLT tests have a mass loss rate that peaks at around 40 g/s.

The ignition times, $t_{CLT,ig}$, of the CLT ceilings (series C) lowers by introducing ceiling intrusions. This time decreases further with the inclusion of more intrusions. Ignition of the ceiling is discussed in more detail in section 3.3.

Based on values reported in the literature for bench-scale apparatus the critical mass loss rate for self-extinction of timber is 3.93 ± 0.45 g/m²s, [21]. Whilst these values are specific to the testing apparatus used, they present a useful comparator value that could indicate the potential for self-extinction. With an exposed surface area of 1.98 m² the critical average mass loss rate measured at the occurrence of full self-extinction of the CLT inside of these compartments is 7.78 ± 0.89 g/s assuming uniform exposure to the CLT surface from the fire. Since the self-extinction observed occurs at one end of the compartment this value of mass loss rate is a lower bound for this threshold. Although Figure 5 shows the total mass loss rate for the entire test setup, at the time of self-extinction the movable fuel load had burnt out and so the majority of mass loss measured is attributable to the CLT ceiling and so this threshold is indicated in Figure 5 for illustration. As can be seen, the self-extinction of the CLT occurs significantly after the total mass loss rate for the entire test setup drops below this critical mass loss rate. Self-extinction of the ceiling will be discussed further in section 3.3.

Table 5 summarises the length of the period in which the fire is in each Mode in the tests reported in this paper. For the timber tests, the time spent in Mode 3 is consistently longer for the same configuration of compartment as the non-combustible ceiling tests. Similarly, the time spent in Mode 2 is consistently shorter. The longer time during which the timber tests are in Mode 3 and the shorter time to transition from Mode 2 to Mode 1 can be attributed to the difference in the thermal inertia of the two ceilings used in these tests, as described in section 2. The higher thermal inertia of the ceiling in the CLT tests results in a slower increase in temperature of the ceiling surface in the case of the CLT as compared to the plasterboard ceiling under the same heat exposure period. Furthermore, the presence of moisture and

incipient pyrolysis reactions will add a further delay to the evolution of the CLT surface temperature. The result is reduced thermal feedback onto the fuel-bed for the CLT ceiling tests before ignition of the CLT. While both ceiling materials facilitate moisture transport, these effects would be expected to be greater in timber meaning that timber would be expected to have larger endothermic losses at the ceiling surface owing to moisture transport from the ceiling surface. Consequently, these results show that the thermal inertia of the ceiling material has a large influence on the spread rates and thus the timescales associated to the transitions from the various modes.

Consistent with Figure 3, the addition of ceiling intrusions (tests B2 and B3) compared to the flat ceiling (B1) reduces the onset times for each of the transitions between the different modes. This behaviour is also consistent with the results seen in the CLT tests, although as will be discussed it is believed that the ceiling intrusions also contribute to an earlier ignition of the CLT.

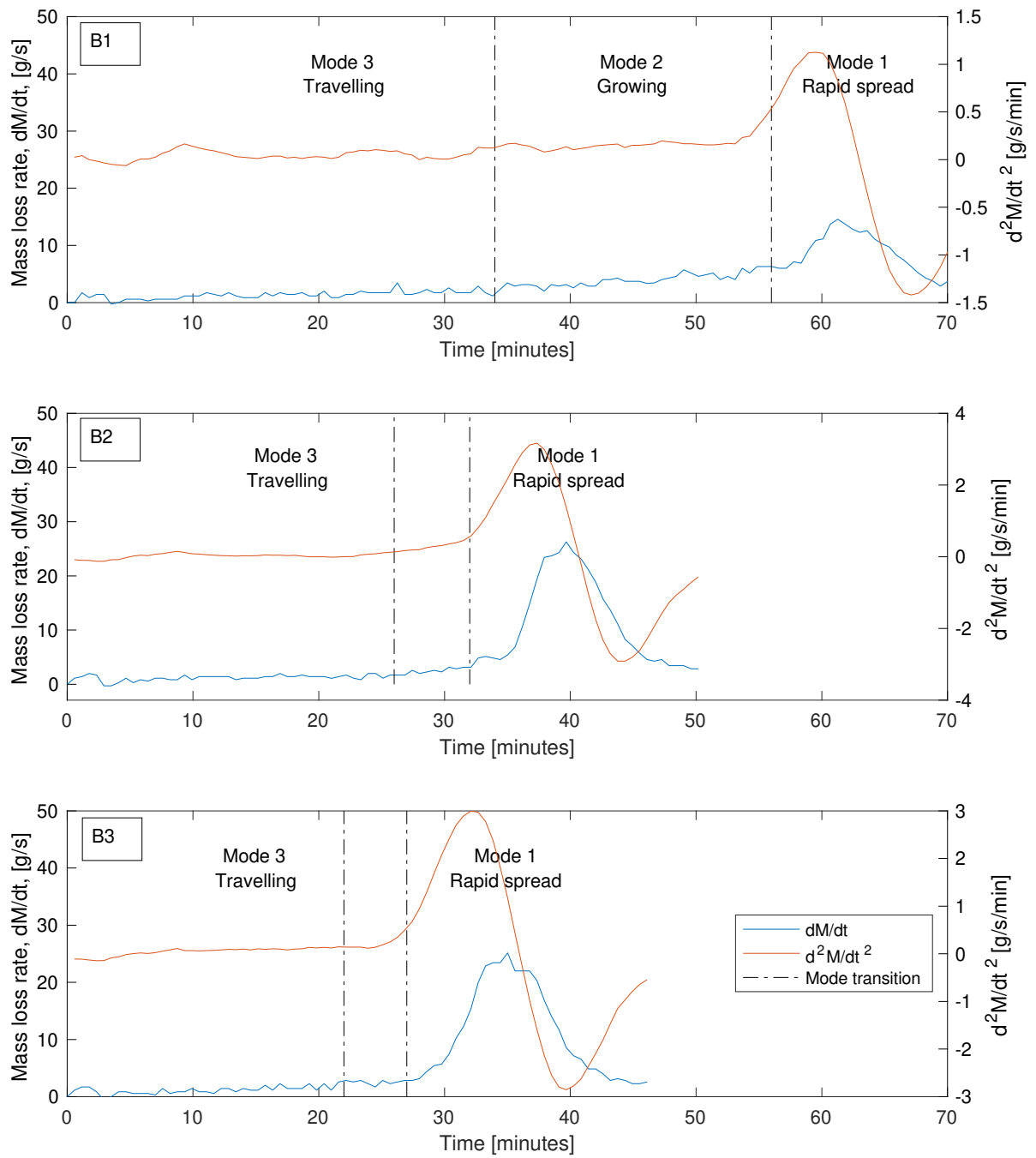


Figure 4. Mass loss rate of the experimental setup with non-combustible ceiling (B1) no ceiling intrusions, (B2) with an edge beam, and (B3) with an edge and a middle beam

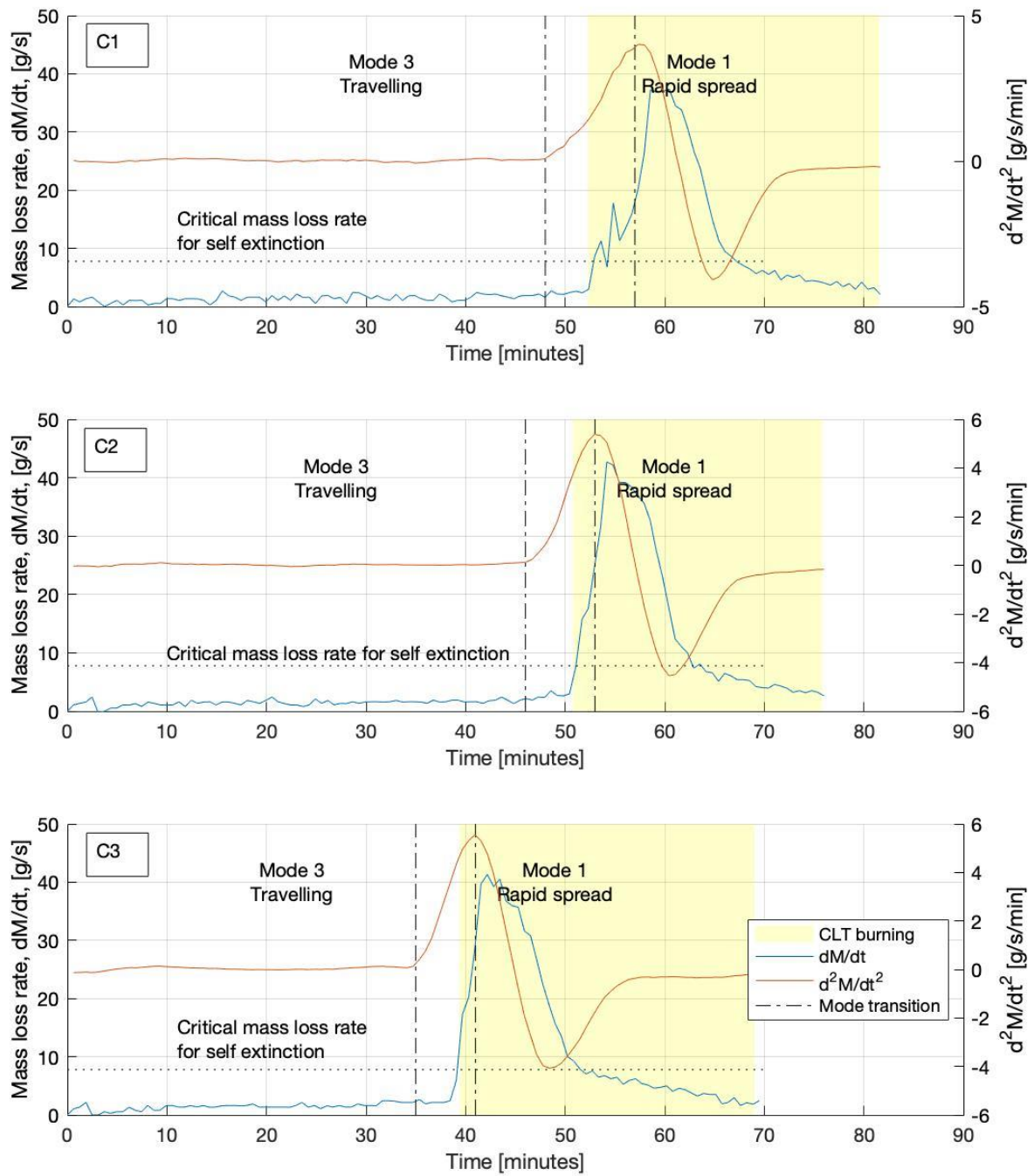


Figure 5. Mass loss rate of the experimental setup with the CLT ceiling (C1) no ceiling intrusions, (C2) with an edge beam, and (C3) with an edge and a middle beam

Table 5. Times at which the fires exhibit the different Modes and the duration in Modes 3 and 2.

	B1	B2	B3	C1	C2	C3
Mode 3 (Travelling)	0 – 34 minutes	0 – 26 minutes	0 – 22 minutes	0 – 48 minutes	0 – 46 minutes	0 – 35 minutes
Mode 2 (Growing)	34 – 56 minutes	26 – 32 minutes	22 – 27 minutes	48 – 57 minutes	46 – 53 minutes	35 – 41 minutes
Mode 1 (Fully developed)	56 minutes – end	32 minutes – end	27 minutes – end	57 minutes – end	53 minutes - end	41 minutes – end
Duration Mode 3	34 minutes	26 minutes	22 minutes	48 minutes	46 minutes	35 minutes
Duration Mode 2	22 minutes	6 minutes	5 minutes	9 minutes	7 minutes	6 minutes

For comparison with the modes identified based on mass loss rates, flame front and burnout location are shown in Figure 6 for the baseline tests and in Figure 7 for the tests with a CLT ceiling. The scattered data in the plots is the raw data derived from the video observations and the solid lines show: 1. a linear fit of the time evolution of the flame front locations for the time duration of each mode; and 2. a linear fit of the burnout front location as a function of time throughout the duration of the test.

In these plots, Mode 3 behaviour is characterised by the parallel progression of the flame front and the burnout location i.e., the burning area of fuel remains constant. This mode is most easily observed in the CLT ceiling compartments (Tests C1 to C3). This is because these tests exhibit Mode 3 behaviour for a longer duration in comparison with tests B1 to B3 (see Table 5 for details). The transition from Mode 3 to Mode 2 and then ultimately to Mode 1 is identifiable as a result of the flame front propagating faster than the burnout front, increasing the total burning area.

The ratios of V_S/V_{BO} , as well as their component velocities for each test are summarised in Table 6. These component velocities may be compared with spread rates reported for travelling fires in the literature, summarised in [14], which range from 0.1 mm/s for fires in the open [39] to 14.5 mm/s to fires in buildings [40].

Spread rates in Mode 3 are relatively consistent between each test, ranging from 9.4 to 16.4 mm/s, comparing favourably with the upper bound reported in the literature. Note that the travelling fire spread rates are very much determined by the specific characteristics of the wood crib. For a travelling fire to occur, there must be minimal external influence on spread and burnout rates. Therefore, the characteristics of the crib determine the propagation rates. The larger the porosity and the less thick a wood crib is the faster the spread rates will be [37]. In the tests reported in this paper, the cribs have a small thickness and a low mass which therefore lends itself to fast spread rates.

Variation in spread rates in Mode 2 between each test is largely attributed to the location of the flame front at the time of transition – when this coincided with spread from one crib to another then the spread rates are lower and since the time in Mode 2 is relatively short, in all but test B1, (Table 5) it is sensitive to this. For this reason, the flame spread rate is only presented for Mode 2 in test B1, which was in Mode 2 for 22 minutes. Spread rates in Mode 1 in all tests are very rapid, above 50 mm/s. The ratio V_S/V_{BO} in Mode 3 in all tests varies between 0.7 and 1.1, growing to between 5.5 and 140.8 in Mode 1.

Burnout location velocities are uniformly higher in the non-combustible tests, as are the spread rates in Mode 1.

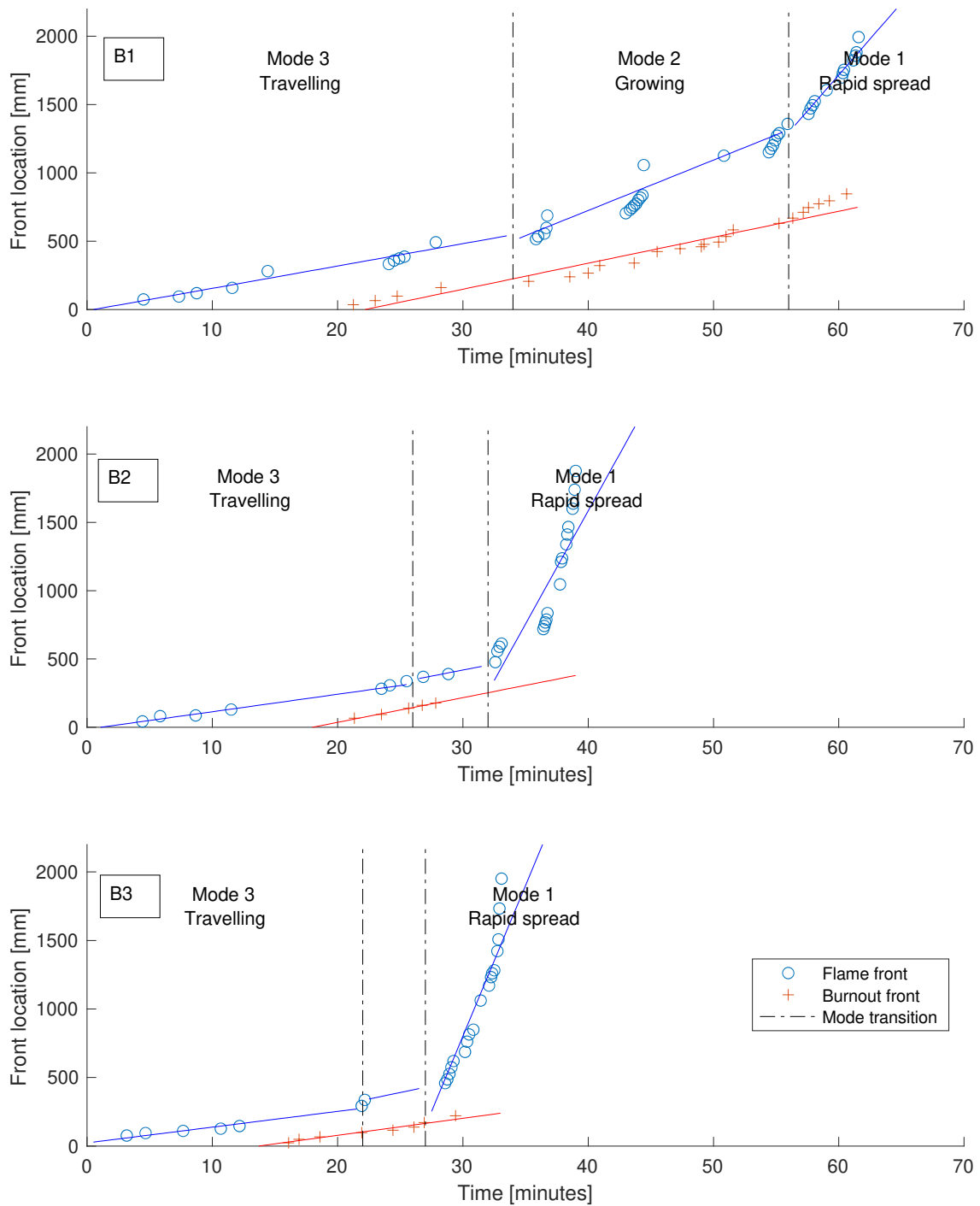


Figure 6. Flame and burnout front location showing modes of flame spread during baseline tests (B1) No ceiling intrusions (B2) Edge beam (B3) Edge and middle beam.

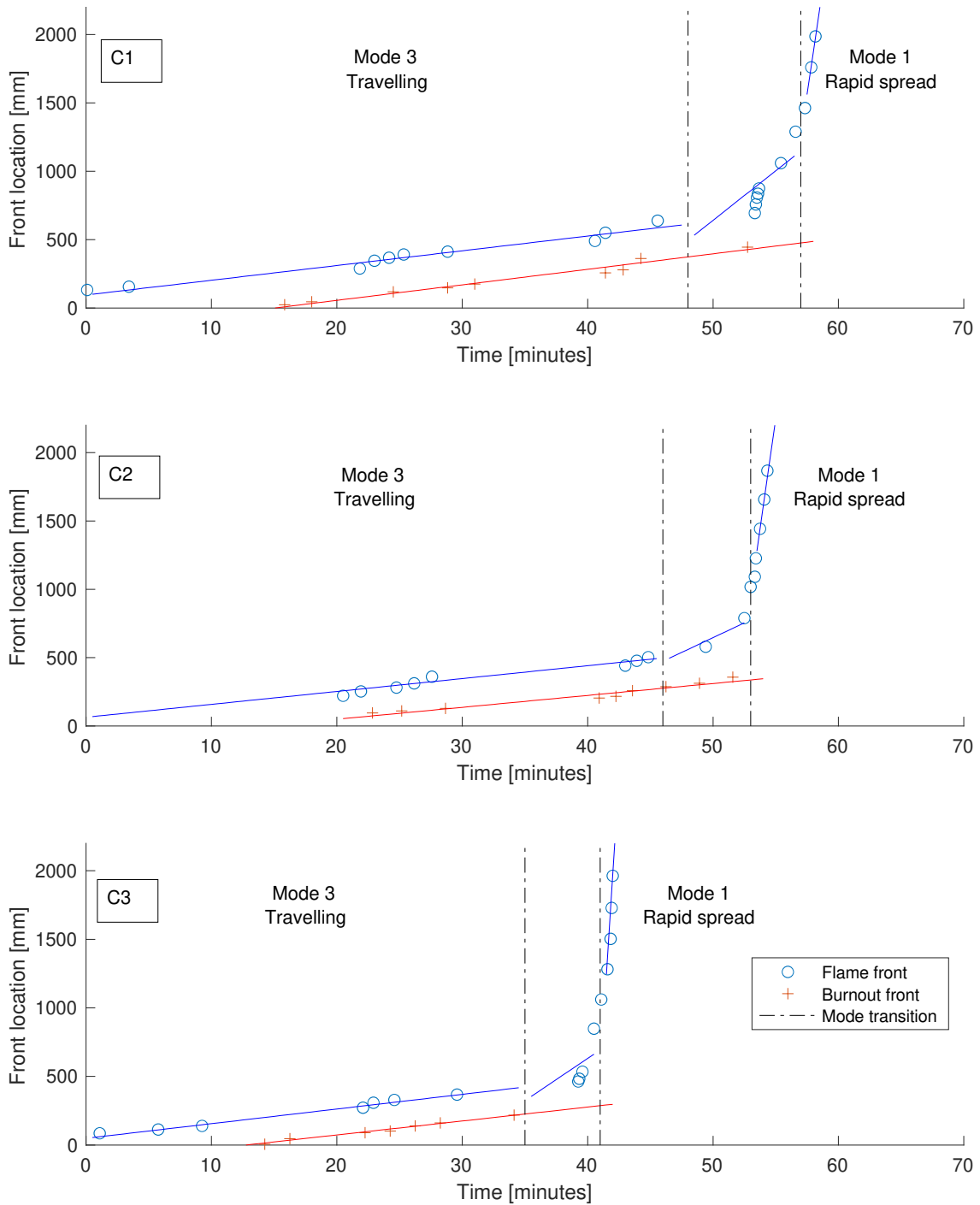


Figure 7. Flame and burnout front location showing modes of flame spread during CLT tests (C1) No ceiling intrusions (C2) Edge beam (C3) Edge and middle beam.

Table 6 – Ratio of flame spread rate to burnout velocity, and spread and burnout rates in each test

		Non combustible			Timber		
		Mode 3	Mode 2	Mode 1	Mode 3	Mode 2	Mode 1
Configuration 1	Ratio V_S/V_{BO}	0.9	1.9	5.5	1.0	-	5.5

	V_S [mm/min]	16.4	36.9	105.4	10.8	-	62.3
	V_{BO} [mm/min]	19			11.3		
Configuration 2	Ratio V_S/V_{BO}	0.7	-	9.2	1.1	-	74.3
	V_S [mm/min]	12.8	-	165.6	9.4	-	646.0
	V_{BO} [mm/min]	18.0			8.7		
Configuration 3	Ratio V_S/V_{BO}	0.9	-	17.7	1.0	-	140.8
	V_S [mm/min]	11.5	-	219.8	10.7	-	1436.0
	V_{BO} [mm/min]	12.4			10.2		

3.2 Heat release rate

The HRR from each test is shown in Figure 8. A higher peak HRR (of almost double) is shown in the two tests B2 and B3 compared with B1. This is attributed to the fact that the fire transitioned to Mode 1 in Test B1 close to the end of the compartment meaning that there were comparatively few cribs burning simultaneously and thus significantly less energy being released at the end of the test. This is also illustrated in the test B1 timeline, Figure 3, where a maximum of 5 cribs are shown to be burning in test B1 compared with 7 or 8 in all other tests.

Peak HRRs are attained earlier for the tests with ceiling intrusions, corresponding to the early onset for the transitions to Mode 2 and then Mode 1 as noted in the previous section. The peak value of HRR is also increased from the baseline tests by almost 100% with the inclusion of the CLT ceiling due to the additional fuel load of the CLT. Similar to the non-CLT tests, introducing ceiling intrusions again leads to an earlier peak in the HRR.

The outcome of containing hot gases with ceiling intrusions leads to a decreased burnout time for all experimental configurations. The time to peak HRR in the baseline tests with ceiling intrusions is shorter than in the CLT tests with ceiling intrusions.

The impact of the CLT on the overall heat released is summarised in Table 7 which shows the total energy released during each fire test. Note the variation in total energy released during the baseline tests, which varies between 95.6 % and 107.1 % of the estimated energy available from the wood cribs reported in section 2, The total energy released during the CLT tests is more consistent from one test to another. The estimated energy available from the wood cribs is therefore used to compare the energy contributed from the CLT ceiling. Based on this the CLT ceiling is estimated to contribute 46 % of the total energy in the CLT compartments regardless of the ceiling configuration. Compared to other observations of the contribution of CLT in full scale tests, where the CLT was estimated to contribute approximately an additional 20 % to 40 % to the internal HRR inside of a fire resistance furnace [41 - 43].

Similar comparisons with full scale open plan compartments in the literature, such as those cited in [7-9] and [33] are not possible since there was no CLT present in these tests. A recent review of large-scale fire tests shows that there are very few with combustible ceilings [17] and indeed the closest comparison in terms of overall behaviour may be made with the Malveira test [8]. However, whilst the comparison is favourable with regards to the identification of the modes observed, the contribution of the cork ceiling to the heat released was not measured or estimated in Malveira. It is anticipated that as other large-scale tests are more fully reported, such as those described in [29, 30], that such comparisons may be possible.

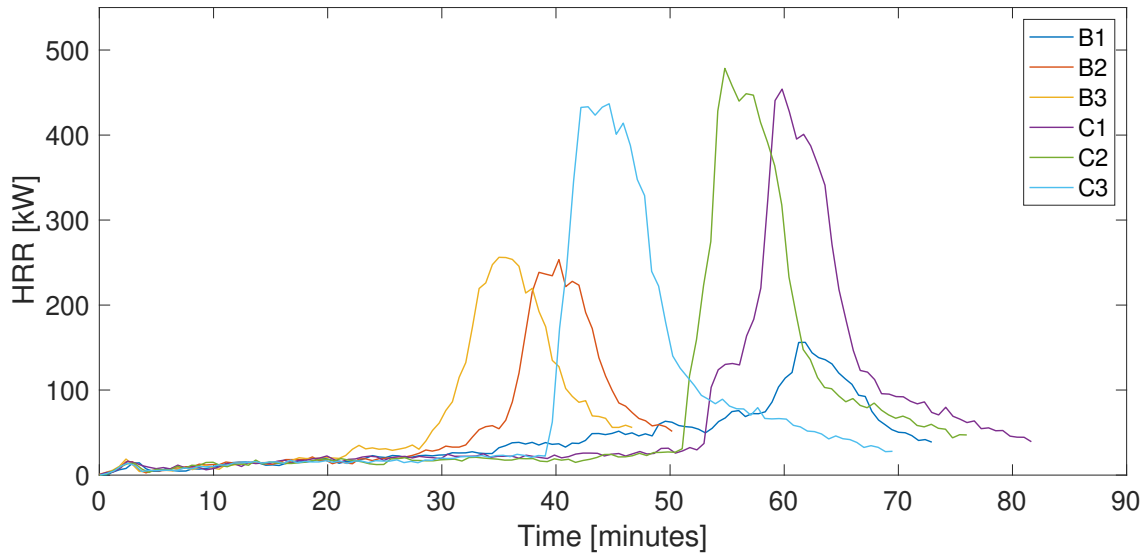


Figure 8 – HRR comparison of each test configuration.

Table 7. Duration and energy released for the fully-developed phase of the compartment fire.

Test Configuration	B1	B2	B3	C1	C2	C3
Total energy released [MJ]	185.93	166.01	177.92	319.49	321.41	319.00
Energy from CLT [MJ]	N/A	N/A	N/A	145.89	147.81	145.4
Approximate percentage of energy from CLT [%]	N/A	N/A	N/A	45.6 %	46 %	45.6 %

3.3 Flame spread on the fuel bed and ignition of the CLT

Ignition is driven by the critical heat flux for ignition $\dot{q}''_{0,ig}$, the minimum incident heat flux necessary to raise the surface temperature of the solid to its ignition temperature, T_{ig} after a delay period. A review of the fundamentals of ignition is provided by Torero [44]. Under standard testing conditions, the critical heat flux and surface ignition temperature for piloted ignition range from 10 kW/m² to 14 kW/m² and 296 to 355 °C, respectively for timber [45, 46]. However, this value is not a true ignition temperature, but a global value used as a reference and that is strongly dependent on both the material properties and local environmental conditions, which greatly differ when comparing the experimental compartment to standard testing apparatus. Parameters which control the ignition temperature include the heat transfer modes (radiation and convection), moisture content, density and thickness of the material as well as the ceiling orientation (i.e. inverted or downward facing, as opposed to facing up). Environmental variables including the flow fields and the oxygen concentration at the surface of the fuel will also have an impact. These variables are necessary conditions to consider in the context of compartment fires, which differ considerably to standard test configurations.

3.3.1 Flame spread on the fuel bed

The relationship between incident heat flux to the surface of the fuel and the location of the flame front is shown in Figures 9 and 10 for the non-combustible ceiling and the CLT ceiling respectively. The scatter plot in these figures shows the distance from the left (the side where ignition of the fuel bed occurred) when looking in through the opening where the incident heat flux imposed onto the fuel-bed surface is equal to or greater than 10 kW/m² (values of the location correspond to the positions of the TSC's at the surface of the fuel bed, with heat fluxes interpolated linearly at additional points every

0.052 m). This value corresponds to the lower bound of critical heat flux for piloted ignition which has been shown to be an upper bound quantity for the rapid flame spread threshold identified from large-scale experiments [10]. The values in Figures 9 and 10 are based on the average heat flux measured at each x-location within the compartment by the TSCs on the floor. The left most location where this magnitude of heat flux is recorded is the first location at which the response of the compartment will begin to significantly influence the burning behaviour of the wood cribs. This is because up until this point the burning behaviour of the wood cribs is controlled by the individual burning rate of each crib and by the ability of the fire to spread from one crib to another. When the external heat flux to the fuel surface exceeds a critical heat flux for rapid flame spread (which is bounded by $\dot{q}''_{0,ig}$) [10], flames will spread rapidly across the surface of the fuel as a result of the combined effects of heating the remaining unburned fuel by the flame heat flux (from the fuel-bed) and an external heat flux arising from the thermal feedback by the ceiling and smoke layer. In the region of the compartment to the left of where this critical heat flux is measured all the movable fuel load will therefore be burning. In some of the test results presented, there are data points within the first 5 minutes of ignition where the heat flux to the fuel at the left side of the compartment is greater than 10 kW/m². This corresponds to the flaming of the kerosene filled pans used to ignite the first row of wood cribs. However there is a significant period after the kerosene has been consumed and during which the heat flux measured is consistently below this value at any point prior to transition to Mode 2.

Note that for test C1 there are comparatively fewer data points presented for the location of the 10 kW/m² position since the transition was so rapid from Mode 3 to Mode 2.

The transition from Mode 3 to Mode 2 is seen to coincide with the time at which the incident radiation from the upper layer to the top of the fuel bed exceeds the critical heat flux for piloted ignition of 10 kW/m². In comparison with previous results presented in this paper, this is seen to correspond well with:

1. a gradual increase in the mass loss rate after a relatively constant period (Figures 4 and 5) and
2. a departure of the burning region from the constant width as shown in Figures 6 and 7.

Both the increase in mass loss rate and the increase in burning width are indicative of transition from Mode 3 behaviour.

A correlation between the position of the heat flux at the level of the top of the fuel bed first exceeding 10 kW/m² and the flame front estimated based on video footage is also clear Figures 9 and 10. Time to transition to Mode 1 in the CLT lined tests is seen to correspond with both a rapid movement of the 10 kW/m² front towards the right hand side of the compartment which also corresponds to the time at which the CLT ceiling starts fully flaming across its surface.

There is a slight delay in the response, with the location of the 10 kW/m² heat flux tracking slightly ahead of the position of the flame front however this is attributable to the means of determining the critical heat flux for piloted ignition, which is based on steady state conditions, whereas the experiments reported in this paper are transient.

A key outcome from this is that (for the 6 experiments presented) the flame front location in Mode 2 and 1 could be determined approximately based on the incident heat flux received at the fuel surface, i.e. $X_{flame\ front} = X(\dot{q}''_{0,ig})$ and when the incident heat flux at the fuel surface exceeds the critical heat flux for piloted ignition the flame spread rate is unlikely to be constant. The constant presence of heat fluxes above $\dot{q}''_{0,ig}$ is therefore a further indication of the transition from Mode 3 to Mode 2. This condition could easily be checked for engineering models which are designed to represent Mode 3 behaviour, such as the various travelling fire methodologies discussed in the introduction, to determine their validity.

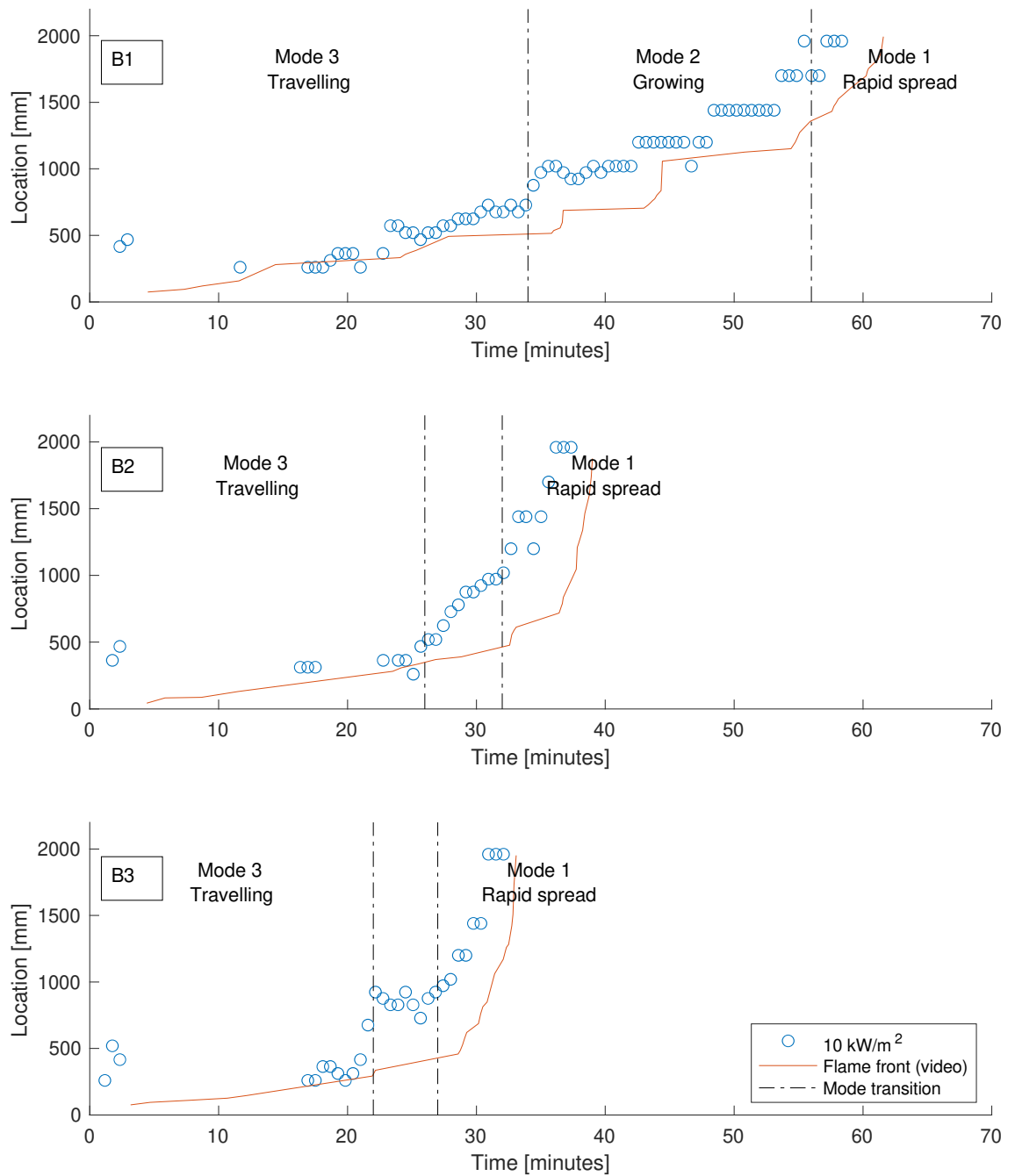


Figure 9. Position of 10 kW/m² heat flux to the floor and the flame front location based on video analysis in compartments with non-combustible ceiling (B1) no ceiling intrusions, (B2) with an edge beam, and (B3) with an edge and a middle beam

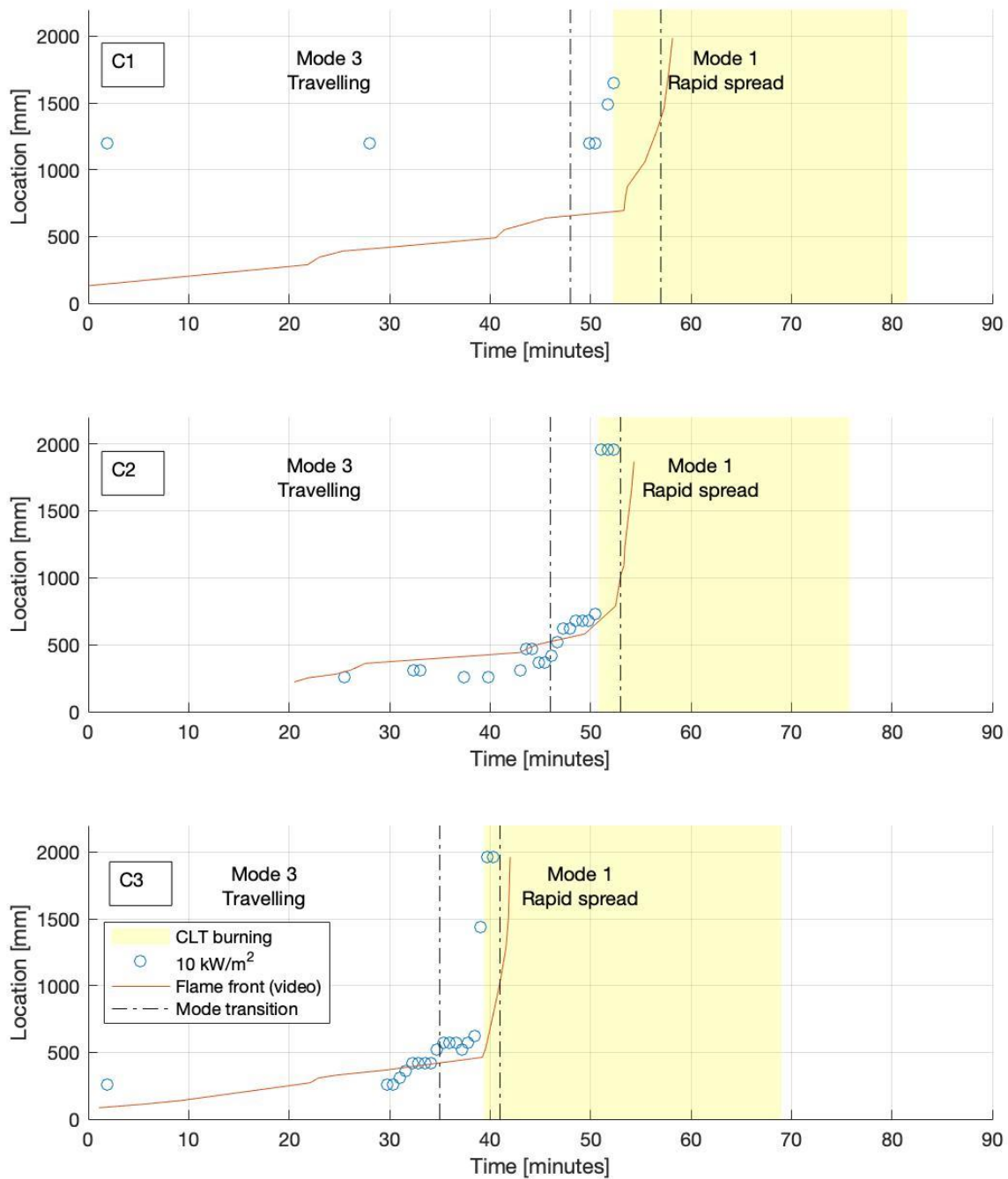


Figure 10. Position of 10 kW/m² heat flux to the floor, flame front location based on video analysis, and CLT burning period in compartments with CLT ceiling (C1) no ceiling intrusions, (C2) with an edge beam, and (C3) with an edge and a middle beam

3.3.2 Ignition of CLT

Ignition of the CLT in the tests occurs upon direct flame impingement from the fire plume onto the surface of the ceiling (the flame acts as a pilot for the ceiling) after a period of preheating. Figure 11 shows incident heat fluxes to the ceiling as a function of time in all tests. Each figure shows the range between the upper and lower bounds of the CLT tests and of the baseline tests of the same configuration.

Time to ignition of the CLT is also shown, as is time to self-extinction of the CLT and burnout of the wood cribs. The lower bound of the critical heat flux for piloted ignition [45, 46] is also indicated as is a threshold heat flux required for self-extinction based on bench scale analysis reported in the literature [21].

For ignition to occur, a flammable gas mixture must exist somewhere in the gas-phase which was then required to be elevated in temperature for the combustion reaction to occur. Once pyrolysis of the CLT occurs, the concentration of volatiles required to attain the lean flammability limit under the specific environmental conditions are required for combustion reaction to occur assuming a strong pilot. This means that pyrolysis reaction rates occur faster than the residence time of the reactants at the CLT surface (i.e. a long enough residence time is required). Ignition of the ceiling occurs in all three of the CLT tests at the same time as the incident heat flux to the ceiling grows rapidly. In all instances a strong comparison may be made between the maximum heat flux to the ceiling and the time to ignition. We present this as a history as opposed to a spatial distribution since after ignition of the ceiling the flame spread across the inverted surface is very rapid. Nevertheless, the location of peak heat flux is approximately coincident with the location of first ignition. For configuration 2 and 3, the peak value of heat flux to the ceiling exceeds the critical heat flux for piloted ignition at approximately the same time as the ignition occurs. However, for configuration 1 there is a delay of several minutes between the peak heat flux exceeding the critical heat flux for piloted ignition and the ignition occurring, shown in Figure 11.

To understand the differences in times to ignition of the CLT in C1 versus C2 and C3, the following key points are highlighted:

- The large size of the openings in configuration 1 enables the hot gases to leave the compartment as fast as air is entrained in. Therefore, the flow fields are dominated by the thermal gradient of the fire source and entrained air, and the flow field is largely momentum-driven [8]. Experimental observations show the gases leaving the compartment without any smoke layer build-up. It is also likely that the flows increase the convective losses and the required external heat flux for ignition.
- As the CLT is heated, initial thermal decomposition of the timber surface induces formation of a char layer. Due to the insulating properties and presence of char, the CLT would have required a higher surface temperature to provide the necessary heat flux to virgin timber to produce sufficient pyrolysis gases for the combustion reaction. In the instances of configuration 2 and 3, preheating of the CLT by the gas inside of the compartment enables the ceiling, or more specifically the location where there is first ignition, to approach thermal equilibrium (i.e. the gradient of temperature behind the heated surface of the timber, dT/dx , does not vary with time,). In these instances, flame impingement provides sufficient energy simply to raise the surface temperature to an ignition temperature, leading to a very short delay time. This explains the very small delay time to ignition on configurations 2 and 3 once the heat flux reaches the critical heat flux for piloted ignition as the solid throughout is already likely closer to a thermal equilibrium than in configuration 1 which has a longer time to ignition after the heat flux reaches the same critical value.
- This is also the reason for the rapid transition from Mode 2 to Mode 1 in configuration 2 and 3 of the baseline and the CLT tests, since confinement of the gas layer has the effect of increasing thermal feedback locally, while also preheating the rest of the fuel.
- In configuration 2 and 3 the ceiling intrusions also have the effect of changing the flow characteristics, resulting in the volatiles being contained for longer within the thicker hot gas layer. This increases the residence time of the pyrolysis gases leading to a faster time to ignition, summarised in Table 4, for the cases with different ceiling intrusions. This was most notable when the middle beam was introduced in configuration 3 which contained the pyrolysis gases in the near field region of the compartment, increasing the residence time and enabling a flammable mixture to form faster.

3.3.3 Self-extinction of CLT

Previous analysis at the bench scale [21] suggests that self-extinction should occur during the fire decay phase once the incident heat flux falls below 45 kW/m^2 . This was determined using a cone heater test configuration within a quiescent atmosphere exposed to a range of constant heat fluxes and thus defines the critical heat flux for self-extinction under an onerous scenario. Self-extinction was observed during each CLT test after the wood crib fuel load was consumed. In all of the CLT tests this occurred first above the area where burnout of the movable fuel load was first observed, when the local contribution to the heat flux to the surface from the burning fuel was removed. The self-extinction progressed across the compartment tracking the burn-out of the movable fuel load. Since the movable fuel load, when several cribs were burning simultaneously, burnt out at approximately the same time the self-extinction on the right-hand side of the CLT ceiling occurred over a large area almost simultaneously and shortly after complete burnout of movable fuel load in the compartment. A short delay was observed between burnout of the movable fuel load and the self-extinction of the CLT ceiling. At the time of self-extinction the peak external heat fluxes to the ceiling in the compartment had dropped below 20 kW/m^2 in test C1, to just above 15 kW/m^2 in test C2, and to just above 10 kW/m^2 in test C3 – all significantly lower than the thresholds identified in [21] meaning that the ceilings will always self-extinguish after the burnout of the movable fuel load in this configuration, which is also in line with the initial conclusions of the full scale STA tests cited earlier [29].

Since the transient heating and cooling rates in compartments leads to in-depth temperature profiles substantially different to bench-scale testing methodologies an extinction threshold based on an empirical value is not universal. Cuevas *et al.* [24] has more recently identified a range of heat fluxes over which self-extinction can be described stochastically under bench scale steady state testing. It was shown that below 30 kW/m^2 , self-extinction is likely to occur, while the probability of extinction is highly unlikely above 40 kW/m^2 . Therefore, the value of 45 kW/m^2 identified in the literature may merely be an indication of the possibility for self-extinction to occur during the decay phase of a fire and this critical value will be dependent on the environmental conditions in the compartment (such as the flow fields), similar to ignition. In all of the CLT tests self-extinction is seen to occur sometime after burnout of the wood cribs and the removal of the external heat flux with no occurrences of partial or complete delamination.

3.3.4 Impact of CLT on the thermal exposure inside of the compartment

Comparison of the heat fluxes to the ceiling between the baseline and the CLT tests in Figure 11 shows that for configurations 2 and 3 the thermal exposure to the ceiling is similar, irrespective of the presence or absence of CLT. This is despite the fact that there is more energy released in the CLT tests, as discussed in section 3.2, suggesting that much of the energy is being consumed outside of the compartment in configurations 2 and 3 with a CLT ceiling.

For B1, the different average heat flux to the ceiling may be attributed to the different numbers of wood cribs that are simultaneously burning, as shown in Figure 3. However, in addition to this, B1 is likely to experience the largest influence from thermal inertia of the ceiling linings since there are no intrusions into the ceiling space to confine the hot gases.

Comparison of the heat fluxes observed with those reported in the literature show that the heat fluxes to the ceiling in Mode 3 in configurations 1 – 3 are very consistent with the lower bound of those observed in large scale experiments displaying the same mode, which are shown to be of the order of between 3 to 25 kW/m^2 , as summarised in [17]. The order of magnitude differences from the Mode 3 to the Mode 1 heat fluxes are also consistent with that seen in large scale experiments, with the Mode 1 values also being at the very lower bound of what might be expected in large scale tests (between 25 to 300 kW/m^2), despite the relatively large fuel load (scaled) in these tests.

The above further supports the conclusion that the scaling methodology captures phenomenologically the same behaviour as is seen in full scale tests.

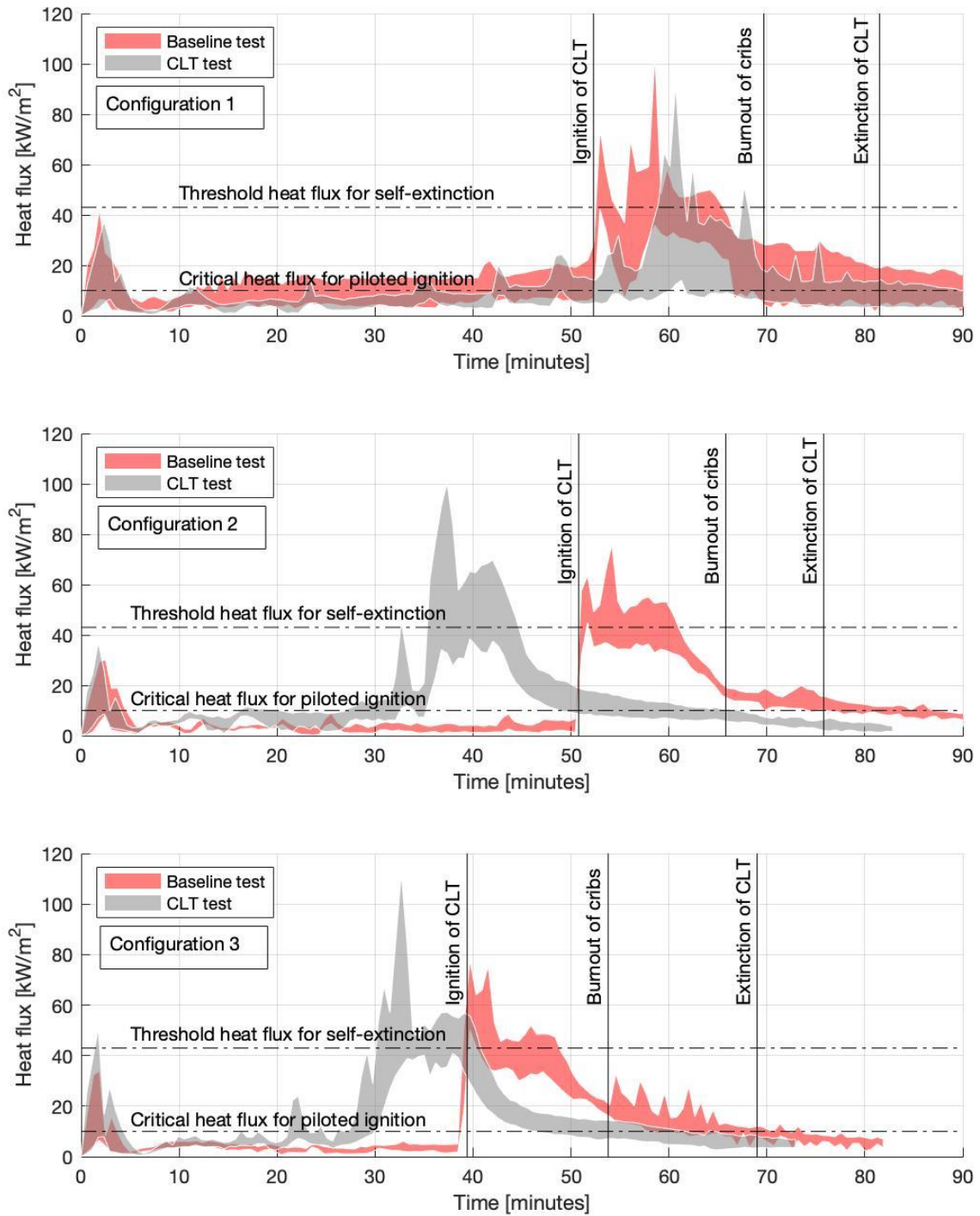


Figure 11 – Range of incident heat flux to ceiling in configuration 1, configuration 2 and configuration 3 in both the baseline and the CLT tests

4 DISCUSSION

4.1 Overall behaviour

All three fire mode behaviours observed (travelling, growing, and fully-developed fires) in full scale prototypes from the literature are identified and quantified in terms of the parameter V_S/V_{BO} for the scaled-down model geometries with non-combustible ceilings. This gives support to the proposed experimental approach for studying these conditions.

While the ratio of V_S/V_{BO} in Mode 3 in all of the tests is shown to be approximately 1, the flame spread rates and the crib burning rates in Mode 3 are shown to be dependent on the overall response of the compartment and the behaviour of the fire inside of the compartments. This dependency is likely enhanced by the relatively thin nature (with 3 layers of sticks) of the wood cribs, which makes their burning behaviour more susceptible to external factors than to the internal crib dynamics by virtue of a larger exposed top surface crib area relative to the total exposed surface area of crib ($A_{S,t}/A_S$) compared to other experiments with more crib layers [37].

The time spent in each Mode differs between the tests with the non-combustible lining and the tests with a combustible lining. In particular, the time spent in Mode 3 is significantly longer in the tests with a CLT ceiling than the tests with the non-combustible ceiling. This is attributable to the relative thermal inertia of the ceiling linings that affects thermal feedback onto the fuel-bed. In the absence of a thick / opaque smoke layer (and assuming in the test setup described in this paper that there is no difference in the smoke layer opacity between the two ceiling materials) the surface temperature of the ceiling as it is heated will be what governs any difference in the interaction between the two types of compartments and the upper surface of the fuel bed.

The time spent in Mode 2 in all of the tests except for the first baseline test is very short, a matter of minutes (Table 5). In the case of the test B1, the longer period spent in Mode 2 may of course be attributable to the larger heat losses than in the other non-combustible ceiling tests. In all the baseline tests, other than the baseline test with no ceiling intrusions, the retention of the hot gas layer, even of a minimal thickness, is sufficient to lead to a significantly faster transition to Mode 1 as a result of the feedback between the fuel bed surface, the hot gas layer and the ceiling lining.

The time spent in Mode 2 in the timber tests is consistently shorter than for the non-combustible ceiling tests. This is particularly the case for C1 in comparison with B1. To understand this, it must be recognised that the transition from the quasi-steady state conditions of Mode 3 to those of Mode 1 represents an overall thermal instability in the compartment fire dynamics. In the combustible ceiling tests, the onset of this instability happens to correspond to the ignition of the CLT ceiling. Once this ignition of the CLT ceiling occurs, rapid flame spread across the ceiling occurs, followed after only a few minutes by rapid flame spread across the fuel bed. In other words, the occurrence of Mode 2 in the CLT ceiling tests is sufficient to rapidly tip the compartment behaviour into a fully developed phase.

The position of the flame front on the floor of the compartment, in Modes 2 and 1, is shown to be largely coincident with the position of the boundary where the external heat flux to the floor exceeds 10 kW/m^2 . There is a minor delay, however this value of the heat flux to the floor corresponds with a lower bound of the critical heat flux for piloted ignition of timber. Noting the nature of the instability represented by Mode 2 and Mode 1 behaviour, once this heat flux to the floor is exceeded, it is very likely that a transition between Modes will occur.

4.2 Ignition of the CLT

Ignition of the CLT follows the same principles as for an upwards facing surface, however in contrast to the upwards facing surface, the boundary conditions inside of the test are driven by the spread of the fire on the fuel bed inside of the compartment. Additionally, the large momentum-driven flows that occur inside of the compartment significantly reduce the residence time of the products of the decomposition of the ceiling as it is heated. This leads to two conditions: firstly, there is a pre-heating of the CLT ceiling as a result of radiation from the flame, and the smoke from the burning fuel as it flows under the ceiling. Under relatively low heat fluxes, the pre-heating allows the CLT to develop a relatively constant temperature gradient. Under continued heating the rate of decomposition of the

timber is constant and momentum-driven flows continue to keep the residence time at the surface low such that a combustible mixture cannot form.

The CLT ceiling leads to a significant increase in the spread rate of the fire in the compartment once ignition of the ceiling occurs, and the compartment subsequently transitions to a fully developed fire. The ignition of CLT is governed by the critical heat flux for ignition, $\dot{q}_{0,ig}''$ and the preheating duration, with a possible delay in the ignition process as discussed in section 3.3.2.

As noted in the timelines of each of the timber tests, local ignition can happen without continued burning of the ceiling, as the ignition consumes all the pyrolyzate. Where there is no retention of a gas layer underneath the timber ceiling, the heat flux to the timber ceiling and thus its decomposition, can exceed the lower bound required for piloted ignition of an upwards facing surface without sustained burning of the timber ceiling. However, so long as the heat flux continues to grow the increased heat flux to a local area of the timber will ultimately be sufficient to push the rate of decomposition above the rate required to sustain burning of the ceiling in the heated region. This represents another type of thermal instability in the overall behaviour of the compartment. In the CLT tests this corresponds with a transition to Mode 2. Once this happens, flame spreads rapidly along the pre-heated timber region. This corresponds to the occurrence of the same instability noted in the previous section, whereby the feedback between the compartment and the top of the fuel bed is sufficient to lead to a transition from Mode 3 to Mode 1. Although the flames along the ceiling are laminar and relatively thin, as shown in Table A2, the additional radiation from the burning timber is sufficient to further increase the heating to the surface of the fuel bed.

The orientation of the ceiling and the residence time of the reactants is likely critical in better understanding or predicting the ignition of the CLT ceiling.

4.3 Self-extinction of the CLT

Self-extinction was observed during each CLT test after the wood crib fuel load was consumed. Self-extinction of the CLT ceiling is the process whereby the rate of decomposition of the CLT is no longer sufficient to sustain the combustion at the surface. This occurs when the external heat flux drops below a certain value required to maintain a through depth penetration of heat sufficient to continue to maintain this rate of decomposition. As discussed in the results section, self-extinction of the timber ceiling in these tests occurs after burnout of the movable fuel load which results in a reduction of \dot{q}_{inc}'' to the ceiling to well below the thresholds for self-extinction identified in the literature [14, 23, 24]. Time scale is a driving factor here, with those limits identified in the literature only indicative of the potential for self-extinction.

As noted in the literature the threshold for self-extinction can be expressed either as a mass loss rate or as a critical heat flux. In either instance, the occurrence of the required conditions is not sufficient to result in self-extinction of the CLT immediately and is only therefore indicative of the potential for self-extinction.

4.4 Impact of ceiling intrusions

The ceiling intrusions are shown to have a non-negligible influence on spread and burnout rates in open plan compartments. The edge beam and the middle beam in the compartment stall the momentum-driven flows and facilitate smoke layer development leading to increased preheating of the fuel-bed. There is also a localised effect as the middle beam enables increased localised heating to a smaller area of the fuel-bed, enhancing local flame spread rates and decreasing the onset time for ignition of the CLT ceiling.

The ceiling intrusions also, by stalling the momentum-driven flow, have the impact of increasing the residence time of the pyrolyzates from the CLT. This contributes to a faster transition from Mode 3 to Mode 2 and then to Mode 1 as the conditions are amenable to earlier ignition of the CLT ceiling. The smaller the reservoir created by the ceiling intrusions, the faster the thermal instabilities that lead to Mode 2 and to Mode 1 can develop.

It must be noted that the impact of ceiling intrusions on the spread rates is quite possibly influenced by the scale of the tests conducted which increases the influence of the differences in thermal inertia of the

ceilings by virtue of a thinner smoke layer. The scale of the compartment geometry likely reduces the time required to transition to rapid flame spread of the fuel bed and in the case of the CLT ceiling tests the ignition of a CLT ceiling. All other behaviour discussed in this paper is consistent with other research reported in the literature and is therefore largely independent, phenomenologically, from the scale of the test conducted.

5 CONCLUSIONS

This article has given an overview of 6 tests which were conducted to determine the influence of an exposed timber ceiling and ceiling intrusions on the fire dynamics in an open plan compartment. The aim of this paper has been to explore some of the phenomena which should be addressed in large scale tests of open plan compartment fires incorporating both non-combustible and combustible ceilings. The tests were conducted at reduced scale and were shown to exhibit similarity in the fire dynamics when contrasted to data from large scale fire tests of similar aspect ratios and configurations in the literature. In that regard, scale testing is shown to be valid with results phenomenologically similar to full scale tests of similar configurations in the literature. The same phenomena are often discussed in this paper as evidenced by more than one experimental result, the intention is that the weight of the evidence presented lends significant support to the conclusions made. This gives further confidence that the phenomena observed here when introducing CLT ceilings are similar to what may be expected at large scale.

When introducing a CLT lining to the ceiling, the same fire Modes are observed as are seen in tests with non-combustible ceilings. It seems likely that open plan timber compartments, on the basis of these tests, should exhibit one or all of travelling, growing and fully developed fire behaviour depending on geometry, fuel load and ventilation. However the transition from Mode 3 to Mode 2 is the onset of an instability in the overall dynamics of the fire which leads rapidly to Mode 1 if sufficient fuel is available. The introduction of a CLT ceiling is seen to increase the rate of transition at this instability.

Flame spread rates on the fuel bed are shown to be most dependent on the interaction with the surrounding compartment when the fire departs from Mode 3 behaviour. When the fire is in Mode 3 behaviour the spread rates are largely independent from the compartment although as a result of the nature of the wood crib used in this test there is some influence on the burning rate of the wood cribs in Mode 3.

Thermal inertia of the ceiling materials is observed to have an influence on flame spread rates. Higher spread rates are seen in the non-combustible tests in comparison with the combustible tests prior to ignition of the CLT ceiling, irrespective of the presence of ceiling intrusions. However, once the CLT ceiling is ignited the flame spread rate in these tests increases significantly compared with the flame spread rate in the non-combustible baseline tests.

The ignition and self-extinction of the CLT ceiling correspond approximately with the criteria for piloted ignition and self-extinction given in the literature. Ignition is delayed as a result of the inverted surface of the ceiling and the momentum-driven flows. Self-extinction is also delayed. While ignition and self-extinction of an inverted timber surface are two areas that require additional further study, it is clear that an inverted timber surface burns in a weaker manner than vertically oriented samples used to characterize ignition and self-extinction of timber.

The above has possible implications for design, suggesting that for open plan timber compartments the ignition delay time of the timber might be a parameter that could be controlled in such a way that it can be balanced against other design constraints and objectives, such as increasing the Available Safe Egress Time or managing the intensity of any structural fires and external flaming in response to increased travel distances and specific tenancy fitouts.

6 ACKNOWLEDGEMENTS

The authors are grateful to Fire Research Group Limited for their support of this project through an FRG Microgrant.

7 REFERENCES

- [1] Thomas, P.H., and Heselden, A.J.M., "Fully developed fires in single compartments", CIB Report No 20. Fire Research Note 923, Fire Research Station, Borehamwood, England, UK, 1972.
- [2] Harmathy, T.Z. "A New Look at Compartment Fires," *Fire Technolgy*, vol. 8, no. 3, pp. 196–217, Aug. 1972.
- [3] McCaffrey, B.J. and Rockett, J.A., "Static Pressure Measurements of Enclosure Fires," *J. Res. Natl. Bur. Stand. (1934).*, vol. 82, no. 2, pp. 107–117, Sep. 1977
- [4] Kawagoe, K., "Fire Behaviour in Rooms - Report No. 27," 1958.
- [5] Harmathy, T. Z., "Design of Buildings for Fire Safety - Part I," *Fire Technol.*, vol. 12, no. 2, pp. 95–108, 1976.
- [6] Torero, J.L., Majdalani, A., Cowlard A., and Abecassis-Empis, C., "Revisiting the Compartment Fire," *Fire Safety Science*, v. 11, 2014
- [7] J.P. Hidalgo, A. Cowlard, C. Abecassis-Empis, C. Maluk & A.H. Majdalani et al. 2017, 'An experimental study of full-scale open floor plan enclosure fires', *Fire Safety Journal*, vol. 89, pp. 22–40, doi:10.1016/j.firesaf.2017.02.002
- [8] J.P. Hidalgo, T. Goode, V. Gupta, A. Cowlard, C. Abecassis-Empis, C. Maluk, J.M. Montalvá, J. Maclean, A. Bartlett, A.F. Osorio, J.L. Torero, The Malveira Fire Test: Full-scale demonstration of fire modes in open-floor plan compartments, *Fire Saf. J.* 108 (2019) 102827, <https://doi.org/10.1016/j.firesaf.2019.102827>.
- [9] Vinny Gupta, Juan P. Hidalgo, Adam Cowlard, Cecilia Abecassis-Empis & Agustin H. Majdalani et al. 2020, 'Ventilation effects on the thermal characteristics of fire spread modes in open-plan compartment fires', *Fire Safety Journal*, pp. 103072, doi:10.1016/j.firesaf.2020.103072
- [10] V. Gupta, A.F Osorio, J.L. Torero, J.P. Hidalgo, Mechanisms of flame spread and burnout in large enclosure fires, *Proc. Comb. Inst.* 38 (2020). <https://doi.org/10.1016/j.proci.2020.07.074>
- [11] V. Gupta, Open-plan compartment fire dynamics, PhD thesis, The University of Queensland 2021
- [12] J. Stern-Gottfried and G. Rein, Travelling fires for structural design—Part I: Literature review, *Fire Saf J.* 54 (2012) 74–85. <https://doi.org/10.1016/j.firesaf.2012.06.003>.
- [13] J. Stern-Gottfried and G. Rein, Travelling fires for structural design—Part II: Design methodology, *Fire Saf J.* 54 (2012) 96–112. <https://doi.org/10.1016/j.firesaf.2012.06.011>.
- [14] E. Rackauskaite, C. Hamel, A. Law, and G. Rein, Improved formulation of travelling fires and application to concrete and steel structures, *Structures* 3 (2015) 250–260. <https://doi.org/10.1016/j.istruc.2015.06.001>.
- [15] M. Heidari, P. Kotsovinos, G. Rein, Flame extension and the near field under the ceiling for travelling fires inside large compartments, *Fire and Materials* 2019 10.1002/fam.2773
- [16] X. Dai, S. Welch, O. Vassart, K. Cábová, L. Jiang, J. Maclean, G. Clifton, A. Usmani, An extended travelling fire method framework for performance based structural design, *Fire Mat.* 44 (2018) 437–457.
- [17] V. Gupta, J.P. Hidalgo, D. Lange, A. Cowlard, C. Abecassis-Empis, J.L. Torero. "A review and analysis of the thermal exposure in large compartment fire experiments", *International Journal of High-Rise Buildings* 10. doi:doi.org/10.21022/IJHRB.2021.10.4.345
- [18] Law, A.; Hadden, R.; Burnout means burnout; SFPE Europe Q1 2017 Issue 5
- [19] Julie Liu, Erica Fischer, Review of large-scale CLT compartment fire tests, *Construction and Building Materials*, 2022, <https://doi.org/10.1016/j.conbuildmat.2021.126099>
- [20] Hangyu Xua, Ian Pope, Vinny Gupta, Jaime Cadena, Jeronimo Carrascal, David Lange, Martyn S. McLaggan, Julian Mendez, Andrés Osorio, Angela Solarte, Diana Soriguer, Jose L. Torero, Felix Wiesner, Abdulrahman Zaben, Juan P. Hidalgo, Large-scale compartment fires to develop a self-extinction design framework for mass timber—Part 1: Literature review and methodology, *Fire Safety Journal* 2022, <https://doi.org/10.1016/j.firesaf.2022.103523>










- [21] R. Emberley, T. Do, J. Yim, J.L. Torero, Critical heat flux and mass loss rate for extinction of flaming combustion of timber, *Fire Saf. J.* 91 (2017) 252-258. <https://doi.org/10.1016/j.firesaf.2017.03.008>.
- [22] Emberley et al. (2017) Description of small and large-scale cross laminated timber tests, *Fire Safety Journal*, 91:327-335. <https://doi.org/10.1016/j.firesaf.2017.03.024>
- [23] Emberley, R., Inghelbrecht, A., Yu, Z., & Torero, J. L. (2017). Self-extinction of timber. *Proceedings of the Combustion Institute*, 36(2), 3055-3062. <https://doi.org/10.1016/j.proci.2016.07.077>
- [24] Cuevas et al. (2020) Flame extinction and burning behaviour of timber under varied oxygen concentrations, *Fire Safety Journal* (in press) <https://doi.org/10.1016/j.firesaf.2020.103087>
- [25] Gorska, C., Hidalgo, J.P., Torero, J.L., Fire dynamics in mass timber compartments, *Fire Safety Journal* 10.1016/j.firesaf.2020.103098
- [26] Hadden, R., Bartlett, I., Hidalgo, J., Santamaria, S., Wiesner, F., Bisby, L., Deeny, S., Lane, B., Effects of exposed cross laminated timber on compartment fire dynamics, *Fire Saf J.* 91 (2017) 480-489. <https://doi.org/10.1016/j.firesaf.2017.03.074>.
- [27] Xu et al. (2019) Exploring the self-extinguishment mechanism of engineered timber in full-scale compartment fires. *Design of Full-Scale Experiments and Preliminary Results. PTEC 2019*
- [28] Robert McNamee, Jochen Zehfuss, Alastair I. Bartlett, Mohammad Heidari, Fabienne Robert, Luke A. Bisby, Enclosure fire dynamics with a cross-laminated timber ceiling, *Fire and Materials*. 2021;45:847–857. DOI: 10.1002/fam.2904
- [29] Danny Hopkin, Michael Spearpoint, Carmen Gorska, Harald Krenn, Tim Sleik, Gordian Stapf, Wojciech Wegrznski, Update on a large-scale CLT experimental campaign for commercial enclosures, *SFPE Europe Q3 2021 Issue 23*
- [30] Large compartment fire experiments: expanding knowledge of building safely with timber, Arup, <https://www.arup.com/perspectives/large-compartment-fire-experiments-expanding-knowledge-of-building-safely-with-timber> accessed 7th January 2022
- [31] Nothard, Sam; Lange, David; Hidalgo, Juan P.; Gupta, Vinny; McLaggan, Martyn S.; The response of exposed timber in open plan compartment fires and its impact on the fire dynamics; 11th International Conference on Structures in Fire (SiF2020); <https://doi.org/10.14264/5d97785>
- [32] J.G. Quintiere, *Fundamentals of Fire Phenomena*, 1st Ed., John Wiley & Sons, Ltd, Chichester, UK, 2006.
- [33] J. Sjöström, E. Hallberg, F. Kahl, A. Temple, J. Andersson, S. Welch, X. Dai, V. Gupta, D. Lange, J.P. Hidalgo, Characterization of TRAvelling FIREs in large compartments, TRAFIR Deliverable Report 2.2, Research Institutes of Sweden, Borås, Sweden, 2019.
- [34] European Committee for Standardisation, EN 1995-1-2: Design of timber structures - Part 1-2: General - Structural fire design.
- [35] Juan P. Hidalgo, Cristian Maluk, Adam Cowlard, Cecilia Abecassis-Empis & Michal Krajcovic et al. 2017, 'A Thin Skin Calorimeter (TSC) for quantifying irradiation during large-scale fire testing', *International Journal of Thermal Sciences*, vol. 112, pp. 383–394, doi:10.1016/j.ijthermalsci.2016.10.013
- [36] Gross, D. (1962). Experiments on the burning of cross piles of wood. *Journal of Research, J. Res. Natl. Bur. Stand.* 66 (1962) 99–105. <https://doi.org/10.6028/JRES.066C.010>.
- [37] V. Gupta, J.L. Torero, J.P. Hidalgo, Burning dynamics and in-depth flame spread of wood cribs in large compartment fires. *Combustion and Flame*, vol. 228, pp. 42–56, doi:10.1016/j.combustflame.2021.01.031
- [38] Hasemi, Y., Yoshida, M., Yokobayashi, Y. and Wakamatsu, Takao, 1997. Flame Heat Transfer And Concurrent Flame Spread In A Ceiling Fire. *Fire Safety Science* 5: 379-390. doi:10.3801/IAFSS.FSS.5-379

- [39] Thomas PH. Some aspects of the growth and spread of fire in the open. *Forestry*1967;40:139–64. <http://dx.doi.org/10.1093/forestry/40.2.139>
- [40] Harold E. Nelson, *Engineering View of the Fire of May 4, 1988 in the First Interstate Bank Building, Los Angeles, California* (NIST IR 89-4061), <https://doi.org/10.6028/NIST.IR.89-4061>
- [41] David Lange, Johan Sjöström , Joachim Schmid , Daniel Brandon , Juan Hidalgo; A Comparison Of The Conditions In A Fire Resistance Furnace When Testing Combustible And Non-Combustible Construction; *Fire Technology* 2020 <https://doi.org/10.1007/s10694-020-00946-6>
- [42] Bartlett A., McNamee R., Robert F., Bisby L. Comparative Energy Analysis from Fire Resistance Tests on Combustible versus Non-Combustible Slabs; *Fire and Materials*
- [43] Węgrzyński W., Turkowski P., Roszkowski P. The discrepancies in energy balance in furnace testing, a bug or a feature? *Fire and Materials* 2019 <https://doi.org/10.1002/fam.2735>
- [44] J.L. Torero, Flaming ignition of solids, in: M.J. Hurley et al. (eds) *SFPE Handbook of Fire Protection Engineering*, Springer, New York, 2011, pp. 633-661.
- [45] D. Drysdale, *An introduction to fire dynamics*, 3rd Ed., John Wiley & Sons, Ltd, Chichester, UK, 2011.
- [46] Bartlett. A, Hadden R., Bisby, L. 2018. A review of factors affecting the burning behaviour of wood. *Fire Technology*, 55, 1-49, 2019.

Appendix ‘A’ – Images of key events

Images of the compartments during the tests are shown in Table A1 and A2 for the baseline and CLT tests respectively. In the baseline tests, Table A1, the images are given for all three fire Modes, as well as the burnout of the fuel. Times at which the images are taken are also provided for information. In the CLT tests, the images are provided during Modes 3 and 1, as well as upon first ignition of the CLT, at a time after the CLT ceiling has fully ignited but before the movable fuel load has become completely involved in the fire, and after burnout of the movable fuel load where it can be clearly seen that the CLT ceiling continues to burn.

Table A1 – Compartment fire evolution and event descriptions for baseline tests.

Event Description	Baseline – Test 1 (B1) No ceiling intrusions	Baseline – Test 2 (B2) Opening Edge Beam	Baseline – Test 3 (B3) Opening Edge and Middle Beam
Mode 3	 13.2 minutes	 15.3 minutes	 16.1 minutes
Mode 2	 43.1 minutes	 32.3 minutes	 23.4 minutes
Mode 1	 60.4 minutes	 37.5 minutes	 32.9 minutes

Burnout



72.9 minutes

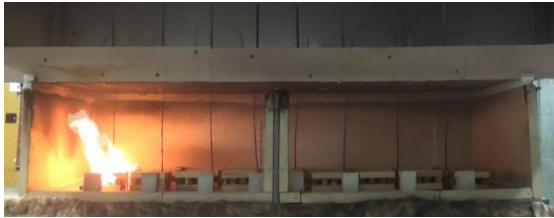
















50.3 minutes



46.2 minutes

Table A2 – Compartment fire evolution and event descriptions for CLT tests.

Event Description	CLT – Test 1 (C1) No ceiling intrusions	CLT – Test 2 (C2) Opening Edge Beam	CLT – Test 3 (C3) Opening Edge and Middle Beam
Mode 3	 <p>15.3 minutes</p>	 <p>12.6 minutes</p>	 <p>11.5 minutes</p>
Ignition of CLT ceiling	 <p>52.3 minutes</p>	 <p>50.8 minutes</p>	 <p>39.4 minutes</p>
CLT ceiling fully flaming	 <p>56.2 minutes</p>	 <p>52.3 minutes</p>	 <p>40.8 minutes</p>

Mode 1	 <p data-bbox="555 389 719 416">58.1 minutes</p>	 <p data-bbox="1135 376 1299 403">53.8 minutes</p>	 <p data-bbox="1715 389 1879 416">41.8 minutes</p>
Burnout	 <p data-bbox="555 687 719 715">69.7 minutes</p>	 <p data-bbox="1135 687 1299 715">65.8 minutes</p>	 <p data-bbox="1715 687 1879 715">53.8 minutes</p>